Reprogramming Yeast Metabolism from Alcoholic Fermentation to Lipogenesis

Article

Cell

Reprogramming Yeast Metabolism from Alcoholic Fermentation to Lipogenesis

Graphical Abstract

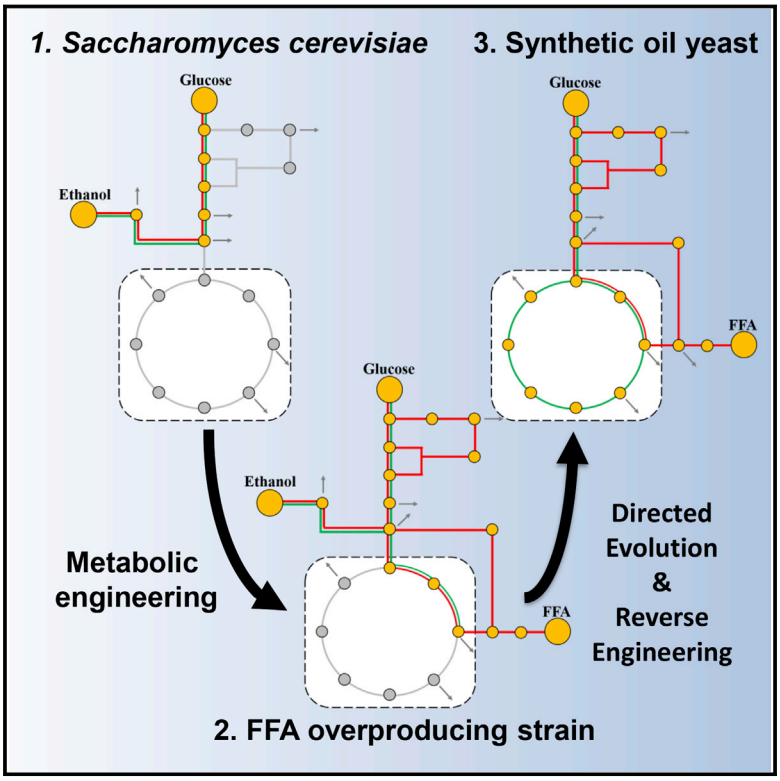

Highlights

- Reconstruction of a heterologous fatty-acid production pathway in yeast
- Growth-coupled design resulted in stable lipogenesis
- Directed evolution enabled complete reprogramming of yeast central metabolism
- Mutations of pyruvate kinase are essential for metabolic flux adaptation

Authors

Tao Yu, Yongjin J. Zhou, Mingtao Huang, Quanli Liu, Rui Pereira, Florian David, Jens Nielsen

Correspondence

nielsenj@chalmers.se

In Brief

Integrated biological redesign, including metabolic rewiring, directed evolution, and bioprocess optimization, allows for reprogramming of *S. cerevisiae* into a synthetic oil yeast.

Yu et al., 2018, Cell *174*, 1549–1558
September 6, 2018
https://doi.org/10.1016/j.cell.2018.07.013

CellPress

Cell

Reprogramming Yeast Metabolism from Alcoholic Fermentation to Lipogenesis

Tao Yu,[1,2,4] Yongjin J. Zhou,[1,2,4,5] Mingtao Huang,[1,2] Quanli Liu,[1,2] Rui Pereira,[1,2] Florian David,[1,2] and Jens Nielsen[1,2,3,6,*]
[1]Department of Biology and Biological Engineering, Chalmers University of Technology, Kemivägen 10, 41296 Gothenburg, Sweden
[2]Novo Nordisk Foundation Center for Biosustainability, Chalmers University of Technology, 41296 Gothenburg, Sweden
[3]Novo Nordisk Foundation Center for Biosustainability, Technical University of Denmark, 2800 Kongens Lyngby, Denmark
[4]These authors contributed equally
[5]Present address: Division of Biotechnology, Dalian Institute of Chemical Physics, Chinese Academy of Sciences, 116023 Dalian, China
[6]Lead Contact
*Correspondence: nielsenj@chalmers.se
https://doi.org/10.1016/j.cell.2018.07.013

SUMMARY

Engineering microorganisms for production of fuels and chemicals often requires major re-programming of metabolism to ensure high flux toward the product of interest. This is challenging, as millions of years of evolution have resulted in establishment of tight regulation of metabolism for optimal growth in the organism's natural habitat. Here, we show through metabolic engineering that it is possible to alter the metabolism of *Saccharomyces cerevisiae* from traditional ethanol fermentation to a pure lipogenesis metabolism, resulting in high-level production of free fatty acids. Through metabolic engineering and process design, we altered subcellular metabolic trafficking, fine-tuned NADPH and ATP supply, and decreased carbon flux to biomass, enabling production of 33.4 g/L extracellular free fatty acids. We further demonstrate that lipogenesis metabolism can replace ethanol fermentation by deletion of pyruvate decarboxylase enzymes followed by adaptive laboratory evolution. Genome sequencing of evolved strains showed that pyruvate kinase mutations were essential for this phenotype.

INTRODUCTION

Engineering microbes for the production of fuels and chemicals enables the replacement of fossil based production and thereby can support the growing population and economy with a lower carbon footprint (Zhou et al., 2016). However, metabolic networks have evolved to have tight regulation to maintain metabolic homeostasis, making it challenging to redirect metabolic fluxes toward desired metabolites (Nielsen and Keasling, 2016). Therefore, many reports on metabolic engineering of microbial cell factories are far away from titer, rate, and yield targets required for establishing commercial processes (Nielsen and Keasling, 2016).

Microbial cell factories are often constructed by establishing a novel biosynthetic pathway without disrupting native metabolic features, which prevents redirection of flux toward desired products. For example, engineering *Saccharomyces cerevisiae*, an ideal cell factory due to its robustness against harsh industrial conditions, for the overproduction of chemicals from glucose is often hampered by its inherent fermentative metabolism where most glucose is shunted toward ethanol (Pronk et al., 1996; Zhou et al., 2016). Fermentative metabolism also predominates under fully aerobic conditions at high sugar concentrations due to the Crabtree effect. Although the Crabtree effect has been extensively studied, its triggering mechanisms remains unknown in *S. cerevisiae* (Hammad et al., 2016), hindering the engineer's endeavor for production of other chemicals than ethanol. As blocking alcoholic fermentation results in growth defects (Flikweert et al., 1999), to support the production of the target product, it is desirable to completely reprogram cellular metabolism.

Recently, microbial fatty acid biosynthesis has attracted much attention for its potential use in generating oleochemicals and biofuels. Among these, free fatty acids (FFAs) are ideal feedstocks for manufacturing of detergents, lubricants, cosmetics, and pharmaceutical ingredients (Tee et al., 2014). Previously, re-engineering of central metabolism and fatty acid biosynthesis has enabled FFA overproduction in microbes such as autotrophic cyanobacteria (0.2 g/L) (Liu et al., 2011), heterotrophic *Escherichia coli* (21. 5 g/L) (Xiao et al., 2016), *S. cerevisiae* (10.4 g/L) (Zhou et al., 2016), and *Yarrowia lipolytica* (10.4 g/L) (Ledesma-Amaro et al., 2016). However, both production titer and yield necessitate further enhancement to enable industrial scale production that is economically feasible.

Here, by simulating the metabolism of oleaginous yeast, we performed major metabolic reprogramming of *S. cerevisiae* toward an efficient lipogenesis metabolism. Central metabolism rewiring resulted in a strain that produced FFAs at a titer of 33.4 g/L, the highest titer reported by microbial fermentation. We further abolished ethanol fermentation in the FFA overproducing strain by laboratory evolution, which led to successful reprograming of ethanol fermentation toward FFA production (Figure 1). Genome sequencing and metabolic characterization showed that the pyruvate kinase mutations were essential to balance glycolysis and cell growth. Based on our findings, we conclude that yeast metabolism, despite millions of years of evolution, is relatively plastic and through a combination of extensive engineering and adaptive laboratory evolution it is possible to

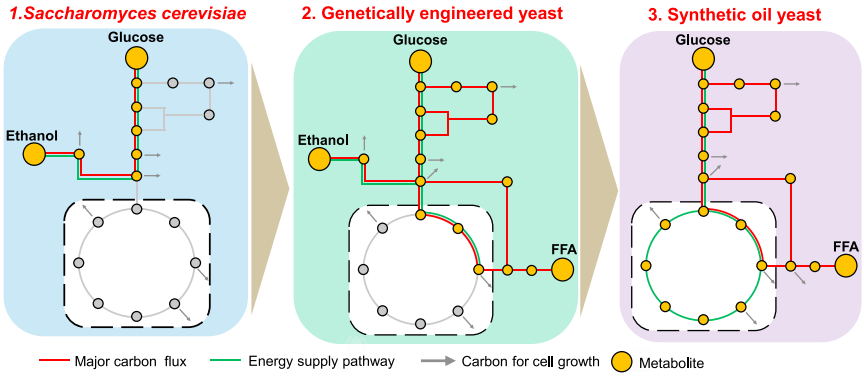

Figure 1. Synthetic Oil Yeast Was Generated by Metabolic Rewiring and Directed Evolution

In wild-type *S. cerevisiae* (1) the "glucose to ethanol" metabolic model dominates the central carbon flux, which also supplies energy for cell growth. To enable a "glucose to oil" metabolic model, an efficient pathway for FFA production was established. To simulate natural oleaginous yeast, ATP citrate lyase (ACL)-derived acetyl-CoA was expressed. By fine-tuning glycolysis, the pentose phosphate pathway (PPP), and the tri-carboxylic acid (TCA) cycle, the supply of the three substrates for FFA biosynthesis, NADPH, ATP, and the precursor acetyl-CoA, were balanced (2). After the abolishment of ethanol production, the cellular fitness was coupled to the new "glucose to oil" metabolic model. After adaptive laboratory evolution, the alcoholic fermentation was successfully reprogrammed into one pure lipogenesis (3).
See also Figure S1.

completely reprogram the functioning of the yeast metabolic network.

RESULTS

To reprogram *S. cerevisiae* into a FFA-producing yeast, we performed three consecutive metabolic rewiring steps (Figure S1A). First, we established an efficient pathway for FFA production. Second, we increased the FAA production capability by ensuring balancing of pathway intermediates, matching the NADPH demand by upregulating the pentose phosphate pathway (PPP) and fine-tuning ATP supply by downregulating the TCA cycle. Third, we abolished ethanol fermentation and performed adaptive laboratory evolution to establish a stable rewired metabolic network (Figures S1B and S1C).

Driving the Carbon Flux by Enhancing the Supply of the Cytosolic Acetyl-CoA

FFA production from glucose can be divided into three modules (Figure S1B): an upstream module of glucose transformation to pyruvate, a middle module of pyruvate conversion to acetyl-CoA, and a downstream module of FFA synthesis from acetyl-CoA. We previously engineered *S. cerevisiae* for FFA over-production and this corresponding strain, YJZ45, that produced up to 7 g/L of FFAs in fed-batch fermentation (Zhou et al., 2016) was our starting strain for this work (Figure S2A). The inherently efficient glycolysis metabolism in yeast from glucose to pyruvate, with the enhanced FFA synthesis from acetyl-CoA in this strain led us to hypothesize that the middle module of pyruvate conversion to acetyl-CoA could be a limiting step for FFA production. As the acetyl-CoA cannot pass through the mitochondria membrane, YJZ45 contains a citrate shuttle, which mainly consists of an ATP:citrate lyase (ACL) that cleaves citrate to oxaloacetate and acetyl-CoA. The provision of cytosolic acetyl-CoA this way, through mitochondrial citrate export, hence also relies on mitochondrial activity for the formation of citrate. We speculated that due to glucose repression of mitochondrial activity there could be a limitation in the formation of citrate in the mitochondria as well as its transport between the mitochondria and the cytosol (Figure 2A). We therefore expressed *PYC1* with the strong *TEF1* promoter (strain Y&Z007), to ensure efficient formation of oxaloacetate required for citrate production and transport. However, using this approach, no obvious improvement in FFA production could be observed. We then assessed whether this strategy could work with an increased supply of malonyl-CoA and therefore overexpressed *ACC1* by replacing its native promoter with the *TEF1* promoter (strain Y&Z009). Here, overexpression of *ACC1* alone gave marginal improvement in FFA production, whereas the combined overexpression of *ACC1* and *PYC1* (strain Y&Z010) improved FFA production by 14% (Figure 2B).

Next, we looked into the subcellular trafficking between mitochondria (TCA cycle) and the cytosol (Figure 2A). In particular, we focused on enhancing mitochondrial citrate synthesis and subcellular trafficking for acetyl-CoA synthesis, a challenging optimization step due to the Crabtree effect in *S. cerevisiae*. The latter means that metabolic flux is predominantly channeled toward ethanol production rather than the TCA cycle at high glucose concentrations, leading to the supply of citrate required for acetyl-CoA synthesis being compromised (Figure 2A). To solve this, we first aimed to enhance mitochondrial pyruvate import. In yeast, the mitochondrial pyruvate carrier (Mpc) is required for mitochondrial pyruvate uptake and is encoded by *MPC1*, *MPC2*, and *MPC3* (Bricker et al., 2012). Here, two complexes exist that contain either Mpc1 and Mpc2 (MPC_{FERM}) or Mpc1 and Mpc3 (MPC_{OX}), with the transport activity of MPC_{OX} being significantly higher than that of MPC_{FERM} (Bender et al., 2015). Thus, we enhanced the expression of *MPC1* and *MPC3* with constitutive promoters to enhance mitochondrial pyruvate import under a high glucose concentration. The resulting strain Y&Z011 produced 1,076 mg/L FFAs in a shake flask cultivation, an 18% improvement compared to its parent strain Y&Z010 (Figure 2B). In mitochondria, the pyruvate dehydrogenase (Pdh) complex and citrate synthase (Cit1) catalyze the consecutive steps of citrate synthesis from pyruvate via acetyl-CoA. The mitochondrial PDH complex consists of an E2 (Lat1) core that binds E1 (Pda1), E3 and protein X (Pdx1) components (Pronk et al., 1996). The E3 and Pda1 subunits have been shown to be inhibited at high glucose concentrations by catabolite repression (Bowman et al., 1992) or through phosphorylation (Oliveira

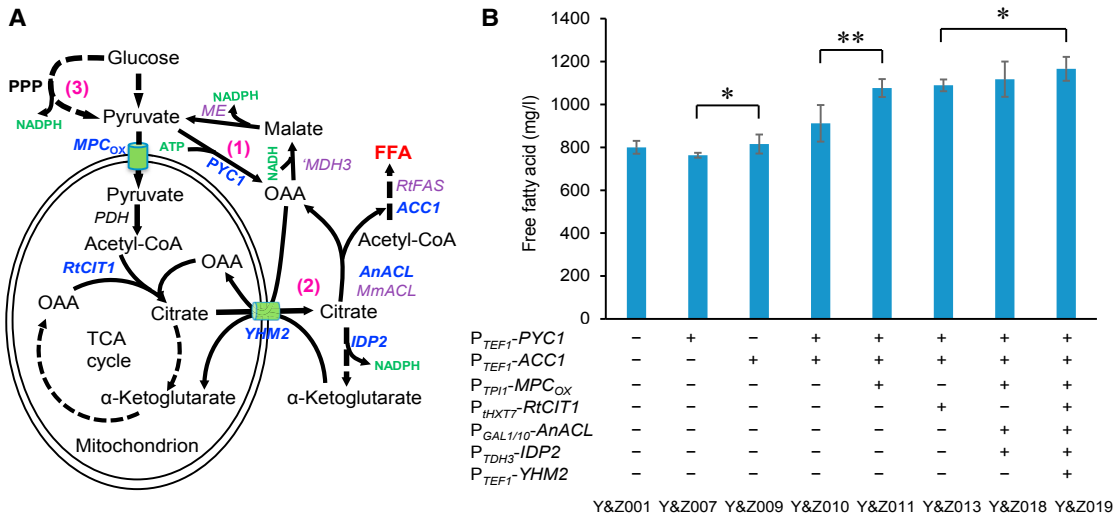

Figure 2. Metabolic Engineering for Enhancing the Supply of Cytosolic Acetyl-CoA

(A) Schematic illustration of the subcellular flux trafficking and engineering targets. Overexpressed genes are shown in blue (in this study) or purple (in the background strain). For more details, see also Figure S1.

(B) FFA production obtained with engineered strains in shake flasks after 72 hr cultivation at 200 rpm, 30°C with 30 g/L glucose. Statistical analysis was performed using one-tailed Student's t test (*$p < 0.05$, **$p < 0.01$, ***$p < 0.001$). All data are presented as mean ± SD of biological triplicates.

See also Figures S2 and S3.

et al., 2012). We thus overexpressed subunits *E3* and mutated *PDA1* (S313A) such that it has abolished regulation by phosphorylation (Oliveira et al., 2012). However, their co-expression resulted in a lower FFA titer with a much lower biomass yield in batch cultivations (Figures S2B and S2C), and as a result, we did not further pursue this strategy. We then aimed to enhance citrate synthesis by overexpressing either the endogenous citrate synthase-encoding gene *ScCIT1* or a heterologous *RtCIT1* from the oleaginous yeast, *Rhodosporidium toruloides*. The *ScCIT1* overexpression (strain Y&Z012) slightly improved FFA production (Figure S3A), while *RtCIT1* overexpression (strain Y&Z013) significantly improved FFA titer by 20% (1,089 mg/L) compared to the parent strain (Y&Z010). We also attempted to enhance mitochondrial oxaloacetate production required for citrate synthesis by relocating the cytosolic *PYC1* within the mitochondrion (m*PYC1*), resulting in a much lower FFA titer and a lower biomass yield (Figures S2B and S2C). The negative affect of *PYC1* relocation from the cytosol to the mitochondria suggests that the mitochondrial pyruvate node is tightly regulated, subsequently altering flux at this node can cause growth defects.

After efficiently channeling carbon flux toward citrate production in the mitochondria via re-engineering MPC_{OX} and *CIT1*, we set out to enhance citrate export from the mitochondria. Previously, the *S. cerevisiae* mitochondrial carrier *YHM2* was characterized as an antiporter for citrate and 2-oxoglutarate (Castegna et al., 2010) and was suggested to also use oxaloacetate in a counter-exchange mechanism. This citrate-2-oxoglutarate transporter acts as a key component of the NADH-NADPH redox shuttle between mitochondria and the cytosol and thus could potentially increase cytosolic NADPH for FFA biosynthesis as well. Therefore, by overexpressing *YHM2* together with $NADP^+$-dependent isocitrate dehydrogenase (*IDP2*) and an *ACL* from *Aspergillus nidulans* (*AnACL*) (Rodriguez et al., 2016b), we were able to improve FFA production up to 1,166 mg/L (strain Y&Z019) (Figures 2B and S3B).

The above engineering strategies resulted in a 46% improvement of FFA production by strain Y&Z019 compared with the starting strain YJZ45 (Figures 2B and S2A). Due to failure in overexpressing the pyruvate dehydrogenase (Pdh) complex, we decided to use glucose-limited fermentations to avoid the Crabtree effect and associated repression of *PDH*. For this purpose, we onward evaluated strain performance in flasks using glucose slow release feed beads. Furthermore, for strain evaluation we shifted to using specific titers, i.e., mg/L/OD_{600} instead of mg/L, with the latter being less sensitive to variations in biomass yield.

Increasing Cofactor NADPH Supply by Fine-Tuning Glycolysis and the PPP Pathway

It has been shown that deletion of *PGI1*, encoding a phosphoglucose isomerase, increases NADPH supply in Corynebacterium glutamicum (Smith et al., 2010) and *E. coli* (Charusanti et al., 2010) via the redirection of glycolytic flux to the pentose phosphate pathway (PPP). However, yeast cells lacking *PGI1* have also been shown to be unable to grow on glucose as a sole carbon source (Aguilera, 1986). Therefore instead of deleting *PGI1*, we downregulated its expression by replacing *PGI1*'s native promoter with a weaker alternative and subsequently screened several different weak promoters for this purpose (Keren et al., 2013) (Figure 3A). In addition, we attempted to enhance PPP flux by overexpressing several genes involved in this pathway, including: *ZWF1*, encoding glucose-6-phosphate dehydrogenase that catalyzes the irreversible and rate limiting

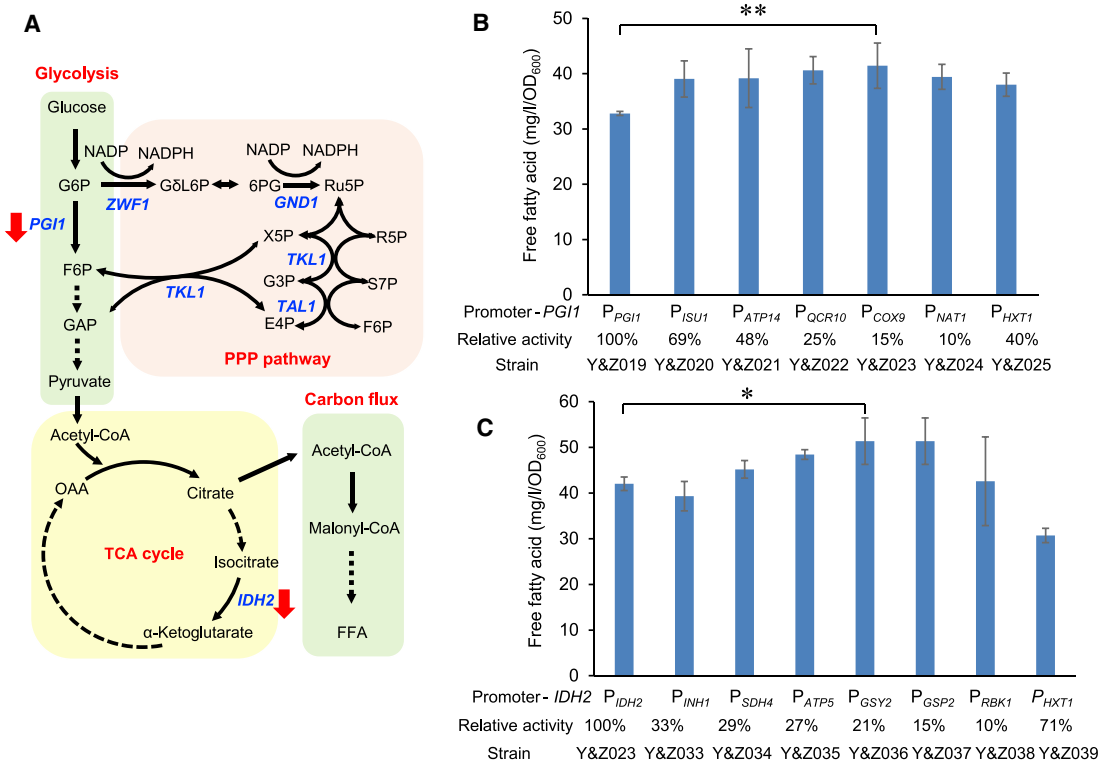

Figure 3. Fine-Tuning the PPP Pathway, TCA Cycle, and Glycolysis for FFA Production

(A) Schematic illustration of metabolic connections between glycolysis, TCA cycle, and the PPP pathway. Overexpressed genes are shown in blue.

(B) Pushing carbon flux into the PPP pathway for improving FFA production by tuning *PGI1* expression.

(C) Fine tuning *IDH2* for optimized TCA flux improved FFA production. The strains were cultivated in shake flasks for 80 hr at 200 rpm, 30°C with glucose feed beads corresponding to 30 g/L glucose. Glucose feed beads release glucose slowly and therefore prevent ethanol production. Statistical analysis was performed using one-tailed Student's t test (*$p < 0.05$, **$p < 0.01$, ***$p < 0.001$). All data represent the mean ± SD of biological triplicates.

See also Figure S3.

first step of PPP and is predominantly responsible for NADPH regeneration from $NADP^+$; *GND1*, encoding the major phosphogluconate dehydrogenase that catalyzes the second oxidative reduction of $NADP^+$ to NADPH; and *TKL1* and *TAL1*, encoding transketolase and transaldolase, respectively, both of which are part of the non-oxidative branch of the PPP. Overexpression of the PPP enzymes together with downregulation of *PGI1* improved FFA production significantly. Specifically, downregulation of *PGI1* expression using the *COX9* promoter (15% activity relative to the native *PGI1* promoter) (Keren et al., 2013) in strain Y&Z023 showed the highest increase in FFA production, with a 28% improvement compared with the parent strain Y&Z019 (Figure 3B).

Carbon Flux Redistribution by Re-engineering the Isocitrate Dehydrogenase Node

In oleaginous fungi, the initiation of lipid overproduction is triggered by impaired activity of the mitochondrial NAD^+-dependent isocitrate dehydrogenase *IDH* (Beopoulos et al., 2009), resulting in citrate export from the mitochondria to the cytosol. To simulate this effect and channel more carbon flux into FFAs, we abolished the *IDH* activity by deleting *IDH1* and/or *IDP1*. However, deletion of *IDH1* (strain Y&Z047) resulted in a much lower FFA titer with reduced biomass yield and double deletion of *IDH* and *IDP1* was lethal (Figures S3C and S3D). We therefore reduced the expression of *IDH* by using weaker promoters (Keren et al., 2013) to fine tune the metabolic flux distribution between ATP generation and increased FFA biosynthesis. Downregulation of *IDH2* under the promoter of *GSY2*, which had 21% activity of the *IDH2* native promoter (strain Y&Z036) (Keren et al., 2013), resulted in a 21% improvement in FFA production compared to the reference strain Y&Z023 (Figure 3C). Interestingly, a similar engineering approach in the strain Y&Z019 showed a marginal effect on FFA production (Figure S3E), which could be attributed to the relatively lower NADPH levels in strain Y&Z019 compared with Y&Z023. This is a good illustration of the challenge with engineering metabolism; it is necessary to combine several different strategies for optimal results, as there is rarely a single bottleneck associated with over-production of a given metabolite, and here NADPH supply, not the flux distribution between ATP generation and precursor supply, might be the limiting step in strain Y&Z019. We also evaluated this strategy in strain Y&Z025, in which the *PGI1* gene is expressed by the *HXT1* promoter, which is induced at high and suppressed at low glucose concentrations. This strain, however, did not result in further improvement of FFA production

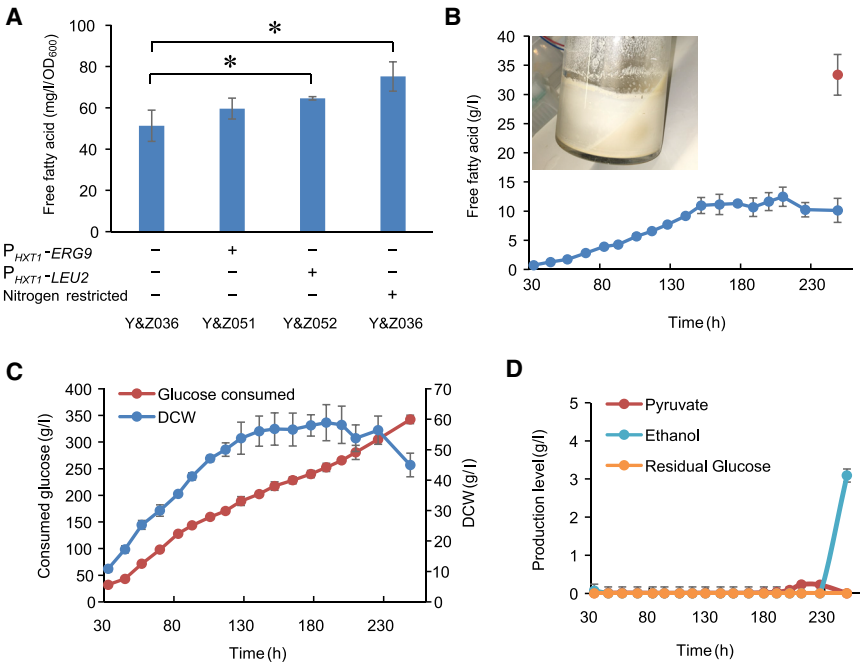

Figure 4. FFA Production Was Further Improved by Growth Decoupling

(A) Limited cell growth by downregulation of essential genes and nitrogen restriction improved FFA production. The strains were cultivated in shake flasks for 80 hr at 200 rpm, 30°C with glucose feed beads (equal to 30 g/L glucose). The glucose feed beads release glucose slowly, to avoid onset of the Crabtree effect. Statistical analysis was performed using one-tailed Student's t test (*$p < 0.05$, **$p < 0.01$, ***$p < 0.001$). All data represent the mean ± SD of biological triplicates.

(B) Fed-batch fermentation of strains Y&Z036 under glucose limited and nitrogen restriction conditions. Time courses of FFA titers (blue symbols) and end point (red symbol) are shown. Red circle, overall FFA production at the end of fermentation (see STAR Methods). Inset photograph: precipitation of FFAs as a result of their overproduction and their adherence to the fermenter inner wall after fed-batch fermentation (further details in Figure S4). The final overall titer therefore also took precipitates into account.

(C) Time courses of dry cell weight (DCW; blue symbols) and consumed glucose (red symbols) during the fermentation.

(D) Time courses of pyruvate (red symbols), ethanol (light blue symbols) and residual glucose (orange symbols) during the fermentation are shown. For (B)–(D), n = 2. Error bars, mean ± SD. See also Figures S3 and S4.

compared with Y&Z036 (Figure S3F) and as the best strain Y&Z042 grows poorly, we selected Y&Z036 for further analysis.

Growth Restrictions for Driving Metabolic Flux toward Fatty Acid Biosynthesis

Lipid overproduction by oleaginous fungi is always initiated by growth stagnation, the latter being triggered by a limitation in nutrients such as nitrogen (Beopoulos et al., 2009). This attribute has been due to the fact that biomass formation competes for carbon and energy. We therefore set out to decouple FFA production from cell growth using two strategies: (1) limiting nitrogen supply, and (2) limiting cell growth by dynamically controlling the expression of essential genes under the *HXT1* promoter, whereby cell growth can be tuned by controlling glucose levels, using glucose feed beads in flask cultures, or using a glucose limited feeding strategy in the fermenter. We selected the essential genes *LEU2* involved in leucine biosynthesis or *ERG9* for ergosterol biosynthesis (Paddon et al., 2013) to demonstrate our concept. Downregulation of *ERG9* (strain Y&Z051) and *LEU2* (strain Y&Z052) improved FFA production by 16% and 25%, respectively, compared to the parent strain Y&Z036 (Figure 4A). The lower biomass yield of Y&Z051 and Y&Z052 suggested that this improvement does indeed result from saving carbon and cofactors for biomass synthesis (Figure S3G). Nitrogen limitation of Y&Z036, however, improved FFA production even more significantly by 47% (75 mg/L/OD_{600} in flask), which was 17% higher increase compared to strain Y&Z052 (Figure 4A). Reducing cell growth in the first strategy was mediated by downregulation of single targets, whereas nitrogen restriction in the second approach induces a broader effect, such as nitrogenous compound recycling and autophagy, which could explain its larger contribution to FFA overproduction (Zhu et al., 2012).

Shake flask tests are useful for strain comparison, however, they underestimate true strain potential due to limited culture controls. Thus, we characterized the best strain, Y&Z036, in a glucose limited and nitrogen restricted fed-batch cultivation, that resulted in production of 33.4 g/L FFAs, representing a 400% improvement over our starting strain and so-far the highest titer reported in literature. This high titer resulted in precipitation of solid FFAs that were stuck on the bioreactor inner wall (Figures 4B, 4C, and S4). Moreover, our engineering not only resulted in an increased final titer of FFAs, but also a 4-fold improvement in yield, which reached 0.1 g FFAs/g glucose corresponding to ~30% of the theoretical yield.

Establishing Pure Lipogenesis by Abolishing Ethanol Fermentation

To evaluate if our novel lipogenesis pathway could replace alcoholic fermentation, we set out to abolish the "glucose-to-ethanol" metabolic pattern and therein evaluate if we could reprogram *S. cerevisiae* as a synthetic oil producing yeast (Figure 1). Pyruvate decarboxylases (Pdc1, Pdc5, and Pdc6) catalyze the decarboxylation of pyruvate to acetaldehydes, which plays a key role in alcoholic fermentation in *S. cerevisiae* (Flikweert et al., 1999). A *pdc* negative strain (*pdc*$^-$ strain), with triple deletion of *PDC1*/5/6, is unable to grow with glucose as the sole carbon source (Flikweert et al., 1996). By deleting all the pdc genes, two important processes are impaired. First, re-oxidation of cytosolic NADH in connection with ethanol fermentation is blocked. Second, the supply of cytosolic acetyl-CoA from

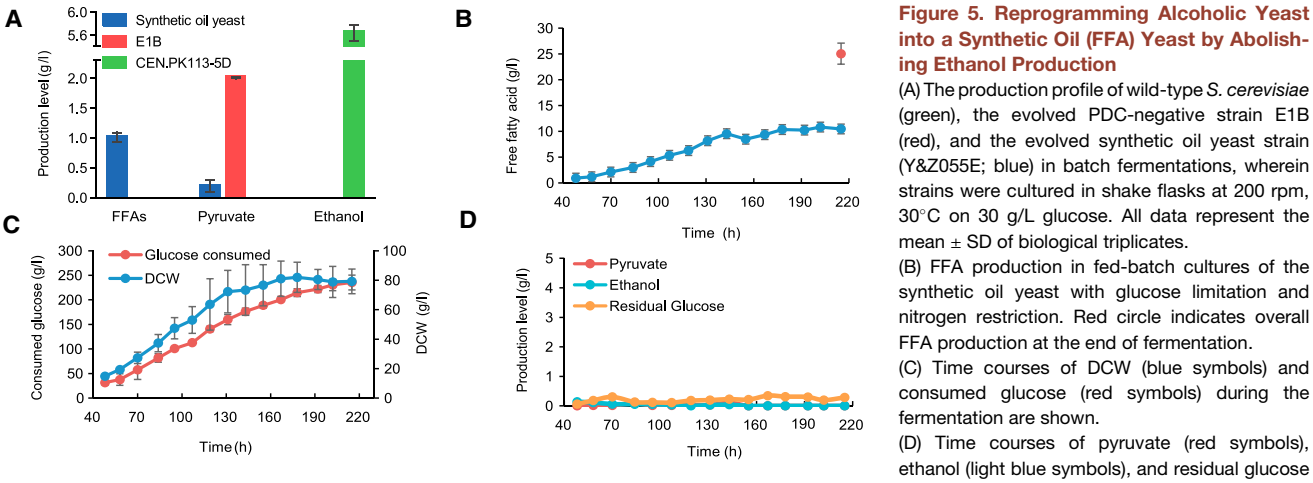

Figure 5. Reprogramming Alcoholic Yeast into a Synthetic Oil (FFA) Yeast by Abolishing Ethanol Production

(A) The production profile of wild-type *S. cerevisiae* (green), the evolved PDC-negative strain E1B (red), and the evolved synthetic oil yeast strain (Y&Z055E; blue) in batch fermentations, wherein strains were cultured in shake flasks at 200 rpm, 30°C on 30 g/L glucose. All data represent the mean ± SD of biological triplicates.

(B) FFA production in fed-batch cultures of the synthetic oil yeast with glucose limitation and nitrogen restriction. Red circle indicates overall FFA production at the end of fermentation.

(C) Time courses of DCW (blue symbols) and consumed glucose (red symbols) during the fermentation are shown.

(D) Time courses of pyruvate (red symbols), ethanol (light blue symbols), and residual glucose (orange symbols) during the fermentation are shown. For (B)–(D), n = 2. Error bars, mean ± SD. See also Figures S5 and S6.

acetaldehyde is blocked, which is required for lysine and cell membrane synthesis (van Maris et al., 2004) (Figure S1B). It was previously shown that adaptive laboratory evolution (ALE) of *pdc*- strains enables restoration of growth on glucose through selection for glucose-derepressed phenotypes (van Maris et al., 2004), but such evolved strains achieve cell growth only through attenuation of glucose uptake, thereby allowing for respiratory metabolism.

Compared to a wild-type strain, the novel lipogenesis pathway in our strain was designed to compensate for this problem due to abolishment of ethanol fermentation. Specifically, (1) our engineering ensures the supply of cytosolic acetyl-CoA by ACL, and (2) the transhydrogenase cycle engineered here can convert excess NADH to NADPH, ensuring sufficient regeneration of NAD^+ (Figure S1B). NADPH here could also be used for FFA production to guarantee the balance of NADP. Thus, cell growth in this context can be coupled to the lipogenesis pathway after blocking ethanol production. Even with these modifications, however, deletion of *pdc* in our FFA overproducing strain Y&Z036 still resulted in lethality in glucose medium. We propose that this growth deficiency is due to metabolic flux imbalance. We therefore used adaptive laboratory evolution (ALE), a method that uses the natural ability of cells to evolve genetic mutations under high selection pressure, to fine tune the carbon flux and restore growth (Figure S5A). This was achieved by starting with growth on ethanol and minimal medium and, during the course of evolution, gradually replacing ethanol with glucose, which led after ~200 generations, to growth on glucose being achieved. The resulting culture produced high levels of FFAs (1.0 g/L) in shake flasks with no detectible level of ethanol (Figure 5A). The FFA overproducing phenotype was clearly maintained during the ALE, indicating our reprogramming of metabolism to support growth in a pdc^- strain had been achieved. In this evolved strain (Y&Z055E), the ratio of unsaturated to saturated fatty acid, especially C16:1 to C16:0, was increased (Figure S5B). It has been shown that stearyl-CoA desaturase introduces the first double bond into saturated fatty acyl-CoA substrates using O_2 and electrons from reduced flavoprotein cytochrome b_5 (Stukey et al., 1990). The two electrons of cytochrome b_5 are supplied by NADH (Lee et al., 2001), suggesting that our synthetic oil yeast handled high NADH pressure by having more fatty acid unsaturation. The culture (Y&Z055E, also herein referred to as "synthetic oil yeast") also accumulated much less pyruvate compared with the strain E1B, an evolved pdc^- strain from the wild-type yeast (Zhang et al., 2015), suggesting that metabolic flux was efficiently channeled toward FFA biosynthesis (Figure 5A). However, Y&Z055E produced higher levels of glycerol and succinate than the E1B strain (Figure S6), further suggesting there was still high NADH pressure in this evolved strain. Subsequent glucose limited, nitrogen-restricted fed-batch cultivation of strain Y&Z055E resulted in a titer of 25 g/L FFAs with a yield comparable to Y&Z036 (Figures 4C, 4D, 5C, and 5D).

Pyruvate Kinase Mutation Is Essential for Restoring Cell Growth to pdc^- Mutants in Glucose

Whole-genome sequencing of three independent clones isolated from the ALE experiment (Figures S2A and S5A) identified 30 mutational events, including large fragments or full chromosome duplications (Figure 6A; Tables S5 and S6). Mutations in pyruvate kinase (*PYK1*) occurred in all three evolved clones: two nonsense mutations (R68* in strain Y&Z056E and K196* in strain Y&Z055E) and a missense mutation (R91I in strain Y&Z054E) that is close to the catalytic pocket shown by structural analysis (Jurica et al., 1998) (Figure S7A). Pyk1, the major pyruvate kinase converting phosphoenolpyruvate (PEP) and ADP to pyruvate and ATP, is tightly regulated and activated by fructose-1,6-bisphosphate (FBP) and considered as a key control point of glycolytic flux (Boles et al., 1997). *PYK2* encodes a second yeast pyruvate kinase which is FBP insensitive (Boles et al., 1997). The evolved strains had much lower total Pyk activity (Figure 7A), but higher Pyk2 activity (Figure 7B) than the wild-type or un-evolved strain, suggesting that Pyk1 activity had been almost abolished and *PYK2* was unregulated in the evolved strains. Consistently, the *PYK2* gene was found to have a copy number increase in the evolved strain

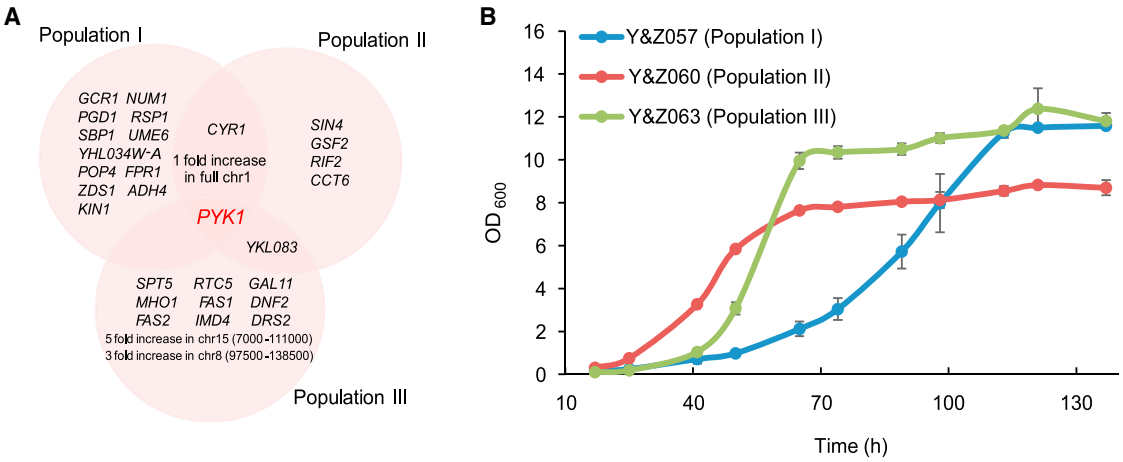

Figure 6. The Genetic Basis for Generating Synthetic Oil Yeast

(A) Venn diagram summarizing the intersection among mutations accumulated in the evolved strains isolated from three distinct evolution experiments. Population I: Y&Z054E (Y&Z057, Y&Z058, and Y&Z059); population II: Y&Z055E (Y&Z060, Y&Z061, and Y&Z062); population III: Y&Z056E (Y&Z063, Y&Z064, and Y&Z065); PYK2 gene had a copy number increase in population III with 5-fold chromosome duplications. For more details see Tables S5 and S6.

(B) Growth curves for the three evolved strains. The strains were cultured in shake flasks at 200 rpm, 30°C with 20 g/L glucose. All data represent the mean ± SD of biological triplicates. Here, the strains Y&Z057, Y&Z060, and Y&Z063 were used from population I, population II, and population III, respectively. See also Figures S5 and S7. The growth curve of the evolved strain, parent strain Y&Z036, and starting strain YJZ45 are shown in Figure S7.

Y&Z056E (Y&Z063, Y&Z064, and Y&Z065) (Figures 6A, 6B, and S7D; Table S6).

Reintroduction of wild-type *PYK1* gene to the evolved strain completely abolished growth in glucose medium (Figure 7C) and downregulation of *PYK1* enabled the growth of the unevolved pdc negative ancestor strain Y&Z053 in high concentrations of glucose (Figure S7B), confirming clear causality between the identified mutation in *PYK1* and the evolved strain's ability to grow on glucose. We hypothesize that metabolic flux adaptation could explain the appearance of mutations in *PYK1* during evolution (Figure 7D). High glycolytic flux during cell growth and especially FFA biosynthesis results in NADH accumulation in the mitochondria and the cytosol, as NAD^+ cannot be regenerated when ethanol production is blocked. The respiratory chain, another NADH oxidation system, is repressed at high glycolytic fluxes due to the Crabtree effect (Bakker et al., 2001). Furthermore, cytosolic NADH oxidation can be a bottleneck, resulting from a higher ratio of unsaturated fatty acids (Figure S5B) and an increased accumulation of glycerol and succinate in the evolved synthetic oil yeast (Figure S6). Furthermore, removal of the engineered transhydrogenase cycle, consisting of the malate enzyme and malate dehydrogenase transforming NADH into NADPH (Zhou et al., 2016), decreases the growth rate of the evolved strain (Figure S7C). These results strongly suggest that high NADH levels was the key pressure to overcome for restoring cell fitness and FFA production. Downregulation of glycolytic flux, by selecting for pyruvate kinase mutations, therefore allows the cell to balance flux through glycolysis with flux toward fatty acid production, and at the same time relieve repression of respiration. Thus, reduced glycolytic flux due to *PYK1* mutations was a way to relieve the Crabtree effect, a phenotype that is consistent with a previous report highlighting that reduced pyruvate kinase activity is sufficient to increase oxygen uptake and respiratory activity (Grüning et al., 2011).

DISCUSSION

Here, we successfully reprogramed the metabolism of *S. cerevisiae* to over-produce FFAs and further demonstrate that, with this reprogramming, it is possible to replace alcoholic fermentation with lipogenesis as the main pathway for metabolizing glucose. From an evolutionary perspective, cellular metabolism has been optimized for conversion of carbon sources into biomass and metabolic products, which can led to growth advantages in their natural habitat. This has resulted in the shaping of central carbon metabolism into several different operational modes, such as the "glucose to ethanol" mode in *S. cerevisiae* and "glucose to oil" mode in oleaginous yeast. Through evolution, these operational modes have become tightly regulated, making it challenging to engineer metabolism for over-production of other metabolites. However, here we demonstrate it is possible to replace the glucose to ethanol metabolism of *S. cerevisiae* with a synthetic pathway for conversion of glucose to FFAs. Further, we demonstrate that with this replacement pathway it is possible to remove ethanol production without abolishing cell growth. With a yield of 0.1 g FFAs/g glucose (~30% of the theoretical yield), the flux directed toward lipogenesis is still not at the level of what is obtained in alcoholic fermentation. However, the complete rewiring of metabolism did not result in a major abolishment of cell growth, meaning that our engineered (and evolved) strains represent a synthetic oil yeast with a stable FFA over-production phenotype. Developing efficient microbial cell factories often requires rewiring of central metabolism, with the desired phenotype being stable for industrial application, something which could be achieved using a

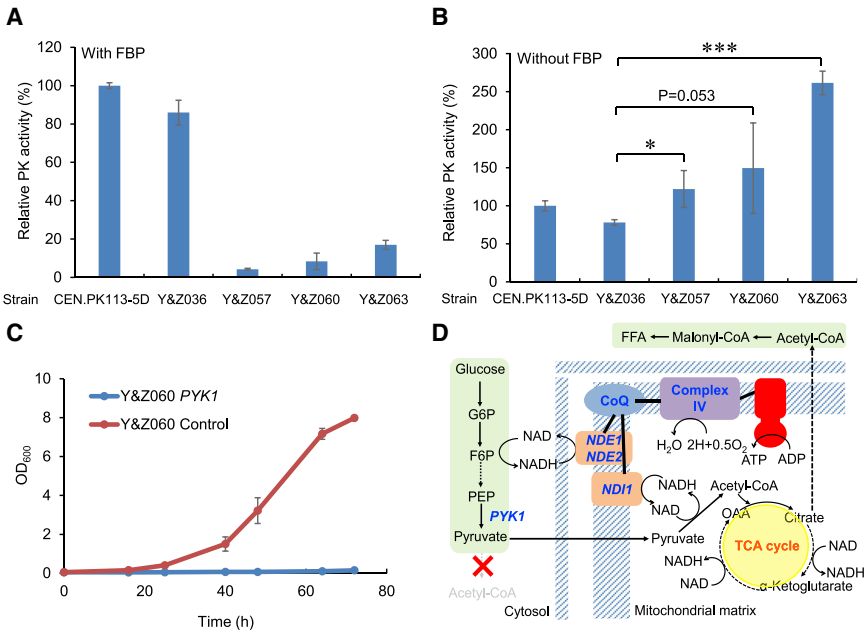

Figure 7. Mutations in Pyruvate Kinase Are Essential for the Evolved Synthetic Oil Yeast Phenotype to Grow on Glucose

(A) The overall activity of pyruvate kinase (PK) in the evolved strains was downregulated. Fructose-1,6-bisphosphate (FBP) was added as an activator of Pyk1.

(B) The activity of *PYK2* in the evolved strains was increased. Here, no FBP was added as an activator. Statistical analysis was performed using one-tailed Student's t test (*$p < 0.05$, **$p < 0.01$, ***$p < 0.001$).

(C) The evolved phenotype was abolished by expression of *PYK1*. The strains were precultured in shake flasks at 200 rpm, 30°C with 20 g/L glucose for 3 days to remove intracellular stores of C2 metabolites, then subcultured in shake flasks at 200 rpm, 30°C with 20 g/L glucose for measurement of optical density at 600 nm (OD_{600}). All data represent the mean ± SD of biological triplicates.

(D) A model depicting why the downregulation of pyruvate kinase might be beneficial for cell growth of the *pdc*$^-$ strain.

See also Figures S6 and S7.

similar approach as outlined here. Furthermore, as we succeeded in redirecting high flux toward cytosolic acetyl-CoA, our engineered strain could also be used for production of other valuable chemicals that are derived from cytosolic acetyl-CoA (van Rossum et al., 2016). We are therefore confident that our engineering efforts can support future developments toward bio-based production of fuels and chemicals.

Compared with traditional design schemes in metabolic engineering where individual genes or modules are tested and then integrated, we coupled the metabolic design to cellular fitness. The lack of sufficient information on enzyme kinetics and metabolic regulation often causes unexpected imbalances in newly designed metabolic networks. In contrast, combining metabolic engineering and evolution allows optimization and balancing of the metabolic network with respect to biosynthesis and cell growth and helps to overcome regulatory constraints. Here, we implemented a metabolic design that allows for coupling of FFA production and cellular growth, enabling high FFA production without penalizing cell growth. As we observed, complete rewiring of central carbon metabolism, wherein ethanol fermentation is replaced with lipogenesis for FFA overproduction, leads to deleterious growth effects as a result of regulatory constraints. However, adaptive laboratory evolution allowed us to overcome this constraint, and through genome-sequencing, we identified the causal mutation. Through a single point mutation in Pyk1, attenuation in the activity of this enzyme was obtained, ensuring a balance between glycolytic flux and fluxes toward FFA production and respiration. Furthermore, the evolved metabolic network showed to be phenotypically stable and can therefore form the basis for commercial microbial-based FFA production.

Our study clearly shows that adaptive laboratory evolution can help establish a balanced metabolic network. We therefore envision that by incorporating adaptive laboratory evolution into future metabolic engineering efforts, using a design-build-evolution-test (DBET) cycle (Nielsen and Keasling, 2016), the process of developing efficient cell factories can be further advanced. Our evolved synthetic oil yeast produces high level of glycerol, subsequently we expect that further rounds of "DBET" cycle could abolish glycerol production with enhanced NADH consumption by the transhydrogenase cycle, or other routes. In other words, we may further couple cell growth to FFA production by better balancing NADH production and consumption through further adaptive laboratory evolution. Furthermore, the "DBET" cycle presented here can easily be established for optimization of other cell factories.

In summary, our results demonstrated that rational design, combined with adaptive laboratory evolution, enabled creation of a synthetic oil yeast with a high production level of FFAs, from the original alcoholic fermentation operation of *S. cerevisiae*. Furthermore, our analysis shows that mutation of pyruvate kinase *PYK1* can result in reduced glycolytic flux, hereby relieving the Crabtree effect. The associated metabolic reprogramming demonstrates that despite millions of years of evolution of *S. cerevisiae,* its metabolism is remarkably plastic, which is also seen in other cellular systems, such as the transformation of metabolism in human cells when they become malignant.

STAR★METHODS

Detailed methods are provided in the online version of this paper and include the following:

- KEY RESOURCES TABLE
- CONTACT FOR REAGENT AND RESOURCE SHARING
- EXPERIMENTAL MODEL AND SUBJECT DETAILS
  - Strains
- METHOD DETAILS
  - Implementation of CRISPR/Cas9 system

SUPPLEMENTAL INFORMATION

Supplemental Information includes seven figures and six tables and can be found with this article online at https://doi.org/10.1016/j.cell.2018.07.013.

ACKNOWLEDGMENTS

We thank Yun Chen, Zhiwei Zhu, and Verena Siewers for helpful discussions. We thank Fredrik Schubert, Stefan Tippmann, and Yun Chen for fermentation support. We thank Kate Campbell for help with final polishing of the manuscript. This research was supported by Knut and Alice Wallenberg Foundation (project no. 2015-0279), the Novo Nordisk Foundation (grant no. NNF10CC1016517), Vetenskapsrådet (grant no. 2015-03852), the Chalmers Area of Advance for Energy, and the Swedish Energy Agency (grant no. 43548-1).

AUTHOR CONTRIBUTIONS

T.Y., Y.J.Z., and J.N. conceived the study. T.Y. and Y.J.Z. designed and performed most of the experiments. T.Y., Y.J.Z., and J.N. analyzed the data. T.Y. and M.H. performed the fermentation and data analysis. Q.L. assisted with experimental performance. R.P. and T.Y. analyzed the genome sequence data. T.Y., Y.J.Z., M.H., Q.L., R.P., F.D., and J.N. wrote the manuscript.

DECLARATION OF INTERESTS

T.Y., Y.J.Z., F.D., and J.N. are listed as co-inventors on a patent application related to fatty acid production. F.D. and J.N. are shareholders in Biopetrolia AB. J.N. is member of Science Advisory Board for Genomatica, Inc., Evolva SA, and Novogy, Inc. All other authors declare no competing financial interests.

Received: March 21, 2018
Revised: May 27, 2018
Accepted: July 9, 2018
Published: August 9, 2018

REFERENCES

Aguilera, A. (1986). Deletion of the phosphoglucose isomerase structural gene makes growth and sporulation glucose dependent in Saccharomyces cerevisiae. Mol. Gen. Genet. *204*, 310–316.

Bakker, B.M., van Maris, A.J., Kötter, P., Luttik, M.A., van Dijken, J.P., and Pronk, J.T. (2001). Stoichiometry and compartmentation of NADH metabolism in Saccharomyces cerevisiae. FEMS Microbiol. Rev. *25*, 15–37.

Bender, T., Pena, G., and Martinou, J.C. (2015). Regulation of mitochondrial pyruvate uptake by alternative pyruvate carrier complexes. EMBO J. *34*, 911–924.

Beopoulos, A., Chardot, T., and Nicaud, J.M. (2009). Yarrowia lipolytica: A model and a tool to understand the mechanisms implicated in lipid accumulation. Biochimie *91*, 692–696.

Boles, E., Schulte, F., Miosga, T., Freidel, K., Schlüter, E., Zimmermann, F.K., Hollenberg, C.P., and Heinisch, J.J. (1997). Characterization of a glucose-repressed pyruvate kinase (Pyk2p) in Saccharomyces cerevisiae that is catalytically insensitive to fructose-1,6-bisphosphate. J. Bacteriol. *179*, 2987–2993.

Bowman, S.B., Zaman, Z., Collinson, L.P., Brown, A.J., and Dawes, I.W. (1992). Positive regulation of the LPD1 gene of Saccharomyces cerevisiae by the HAP2/HAP3/HAP4 activation system. Mol. Gen. Genet. *231*, 296–303.

Bricker, D.K., Taylor, E.B., Schell, J.C., Orsak, T., Boutron, A., Chen, Y.C., Cox, J.E., Cardon, C.M., Van Vranken, J.G., Dephoure, N., et al. (2012). A mitochondrial pyruvate carrier required for pyruvate uptake in yeast, Drosophila, and humans. Science *337*, 96–100.

Castegna, A., Scarcia, P., Agrimi, G., Palmieri, L., Rottensteiner, H., Spera, I., Germinario, L., and Palmieri, F. (2010). Identification and functional characterization of a novel mitochondrial carrier for citrate and oxoglutarate in Saccharomyces cerevisiae. J. Biol. Chem. *285*, 17359–17370.

Charusanti, P., Conrad, T.M., Knight, E.M., Venkataraman, K., Fong, N.L., Xie, B., Gao, Y., and Palsson, B.O. (2010). Genetic basis of growth adaptation of Escherichia coli after deletion of pgi, a major metabolic gene. PLoS Genet. *6*, e1001186.

Deatherage, D.E., and Barrick, J.E. (2014). Identification of mutations in laboratory-evolved microbes from next-generation sequencing data using breseq. Methods Mol. Biol. *1151*, 165–188.

Flikweert, M.T., Van Der Zanden, L., Janssen, W.M., Steensma, H.Y., Van Dijken, J.P., and Pronk, J.T. (1996). Pyruvate decarboxylase: an indispensable enzyme for growth of Saccharomyces cerevisiae on glucose. Yeast *12*, 247–257.

Flikweert, M.T., de Swaaf, M., van Dijken, J.P., and Pronk, J.T. (1999). Growth requirements of pyruvate-decarboxylase-negative Saccharomyces cerevisiae. FEMS Microbiol. Lett. *174*, 73–79.

Grüning, N.M., Rinnerthaler, M., Bluemlein, K., Mülleder, M., Wamelink, M.M.C., Lehrach, H., Jakobs, C., Breitenbach, M., and Ralser, M. (2011). Pyruvate kinase triggers a metabolic feedback loop that controls redox metabolism in respiring cells. Cell Metab. *14*, 415–427.

Hammad, N., Rosas-Lemus, M., Uribe-Carvajal, S., Rigoulet, M., and Devin, A. (2016). The Crabtree and Warburg effects: Do metabolite-induced regulations participate in their induction? Biochim. Biophys. Acta *1857*, 1139–1146.

Jenjaroenpun, P., Wongsurawat, T., Pereira, R., Patumcharoenpol, P., Ussery, D.W., Nielsen, J., and Nookaew, I. (2018). Complete genomic and transcriptional landscape analysis using third-generation sequencing: a case study of Saccharomyces cerevisiae CEN.PK113-7D. Nucleic Acids Res. *46*, e38.

Jeude, M., Dittrich, B., Niederschulte, H., Anderlei, T., Knocke, C., Klee, D., and Büchs, J. (2006). Fed-batch mode in shake flasks by slow-release technique. Biotechnol. Bioeng. *95*, 433–445.

Jurica, M.S., Mesecar, A., Heath, P.J., Shi, W., Nowak, T., and Stoddard, B.L. (1998). The allosteric regulation of pyruvate kinase by fructose-1,6-bisphosphate. Structure *6*, 195–210.

Keren, L., Zackay, O., Lotan-Pompan, M., Barenholz, U., Dekel, E., Sasson, V., Aidelberg, G., Bren, A., Zeevi, D., Weinberger, A., et al. (2013). Promoters maintain their relative activity levels under different growth conditions. Mol. Syst. Biol. *9*, 701.

Langmead, B., and Salzberg, S.L. (2012). Fast gapped-read alignment with Bowtie 2. Nat. Methods *9*, 357–359.

Ledesma-Amaro, R., Dulermo, R., Niehus, X., and Nicaud, J.M. (2016). Combining metabolic engineering and process optimization to improve production and secretion of fatty acids. Metab. Eng. *38*, 38–46.

Lee, J.S., Huh, W.K., Lee, B.H., Baek, Y.U., Hwang, C.S., Kim, S.T., Kim, Y.R., and Kang, S.O. (2001). Mitochondrial NADH-cytochrome b(5) reductase plays a crucial role in the reduction of D-erythroascorbyl free radical in Saccharomyces cerevisiae. Biochim. Biophys. Acta *1527*, 31–38.

Liu, X., Sheng, J., and Curtiss, R., 3rd. (2011). Fatty acid production in genetically modified cyanobacteria. Proc. Natl. Acad. Sci. USA *108*, 6899–6904.

Mans, R., van Rossum, H.M., Wijsman, M., Backx, A., Kuijpers, N.G.A., van den Broek, M., Daran-Lapujade, P., Pronk, J.T., van Maris, A.J.A., and Daran, J.M.G. (2015). CRISPR/Cas9: a molecular Swiss army knife for simultaneous introduction of multiple genetic modifications in Saccharomyces cerevisiae. FEMS Yeast Res. *15*, S253.

Mikkelsen, M.D., Buron, L.D., Salomonsen, B., Olsen, C.E., Hansen, B.G., Mortensen, U.H., and Halkier, B.A. (2012). Microbial production of indolylglucosinolate through engineering of a multi-gene pathway in a versatile yeast expression platform. Metab. Eng. *14*, 104–111.

Nielsen, J., and Keasling, J.D. (2016). Engineering cellular metabolism. Cell *164*, 1185–1197.

Oliveira, A.P., Ludwig, C., Picotti, P., Kogadeeva, M., Aebersold, R., and Sauer, U. (2012). Regulation of yeast central metabolism by enzyme phosphorylation. Mol. Syst. Biol. *8*, 623.

Paddon, C.J., Westfall, P.J., Pitera, D.J., Benjamin, K., Fisher, K., McPhee, D., Leavell, M.D., Tai, A., Main, A., Eng, D., et al. (2013). High-level semi-synthetic production of the potent antimalarial artemisinin. Nature *496*, 528–532.

Pronk, J.T., Yde Steensma, H., and Van Dijken, J.P. (1996). Pyruvate metabolism in Saccharomyces cerevisiae. Yeast *12*, 1607–1633.

Reid, R.J., Sunjevaric, I., Keddache, M., and Rothstein, R. (2002). Efficient PCR-based gene disruption in Saccharomyces strains using intergenic primers. Yeast *19*, 319–328.

Rodriguez, S., Denby, C.M., Van Vu, T., Baidoo, E.E.K., Wang, G., and Keasling, J.D. (2016b). ATP citrate lyase mediated cytosolic acetyl-CoA biosynthesis increases mevalonate production in Saccharomyces cerevisiae. Microb. Cell Fact. *15*, 48.

Smith, K.M., Cho, K.M., and Liao, J.C. (2010). Engineering Corynebacterium glutamicum for isobutanol production. Appl. Microbiol. Biotechnol. *87*, 1045–1055.

Stukey, J.E., McDonough, V.M., and Martin, C.E. (1990). The OLE1 gene of Saccharomyces cerevisiae encodes the delta 9 fatty acid desaturase and can be functionally replaced by the rat stearoyl-CoA desaturase gene. J. Biol. Chem. *265*, 20144–20149.

Tee, T.W., Chowdhury, A., Maranas, C.D., and Shanks, J.V. (2014). Systems metabolic engineering design: fatty acid production as an emerging case study. Biotechnol. Bioeng. *111*, 849–857.

van Maris, A.J.A., Geertman, J.M.A., Vermeulen, A., Groothuizen, M.K., Winkler, A.A., Piper, M.D.W., van Dijken, J.P., and Pronk, J.T. (2004). Directed evolution of pyruvate decarboxylase-negative Saccharomyces cerevisiae, yielding a C2-independent, glucose-tolerant, and pyruvate-hyperproducing yeast. Appl. Environ. Microbiol. *70*, 159–166.

van Rossum, H.M., Kozak, B.U., Pronk, J.T., and van Maris, A.J.A. (2016). Engineering cytosolic acetyl-coenzyme A supply in Saccharomyces cerevisiae: Pathway stoichiometry, free-energy conservation and redox-cofactor balancing. Metab. Eng. *36*, 99–115.

Varman, A.M., He, L., You, L., Hollinshead, W., and Tang, Y.J.J. (2014). Elucidation of intrinsic biosynthesis yields using 13C-based metabolism analysis. Microb. Cell Fact. *13*, 42.

Verduyn, C., Postma, E., Scheffers, W.A., and Van Dijken, J.P. (1992). Effect of benzoic acid on metabolic fluxes in yeasts: a continuous-culture study on the regulation of respiration and alcoholic fermentation. Yeast *8*, 501–517.

Xiao, Y., Bowen, C.H., Liu, D., and Zhang, F. (2016). Exploiting nongenetic cell-to-cell variation for enhanced biosynthesis. Nat. Chem. Biol. *12*, 339–344.

Yu, T., Zhou, Y.J.J., Wenning, L., Liu, Q., Krivoruchko, A., Siewers, V., Nielsen, J., and David, F. (2017). Metabolic engineering of Saccharomyces cerevisiae for production of very long chain fatty acid-derived chemicals. Nat. Commun. *8*, 15587.

Zhang, Y., Liu, G., Engqvist, M.K.M., Krivoruchko, A., Hallström, B.M., Chen, Y., Siewers, V., and Nielsen, J. (2015). Adaptive mutations in sugar metabolism restore growth on glucose in a pyruvate decarboxylase negative yeast strain. Microb. Cell Fact. *14*, 116.

Zhou, Y.J., Buijs, N.A., Zhu, Z., Qin, J., Siewers, V., and Nielsen, J. (2016). Production of fatty acid-derived oleochemicals and biofuels by synthetic yeast cell factories. Nat. Commun. *7*, 11709.

Zhu, Z., Zhang, S., Liu, H., Shen, H., Lin, X., Yang, F., Zhou, Y.J., Jin, G., Ye, M., Zou, H., and Zhao, Z.K. (2012). A multi-omic map of the lipid-producing yeast Rhodosporidium toruloides. Nat. Commun. *3*, 1112.

STAR★METHODS

KEY RESOURCES TABLE

REAGENT or RESOURCE	SOURCE	IDENTIFIER
Chemicals, Peptides, and Recombinant Proteins		
D-Fructose 1,6-bisphosphate trisodium salt hydrate 38099-82-0	Sigma	F6803-1G; CAS: 38099-82-0
Critical Commercial Assays		
PrimeStar DNA polymerase	TaKaRa Bio	Cat#R010A
Phusion High-Fidelity DNA Polymerase	Thermoscientific	REF: F-530L
GeneJET gel Extraction Kit	Thermoscientific	REF: K0692
GeneJET Plasmid Miniprep kit	Thermoscientific	REF: K0503
Gibson Assembly Cloning Kit	NEB	E2611L
Pyruvate Kinase (PK) Assay Kit	Abcam	ab83432
Piece BCA Protein Assay Kit	Thermoscientific	Prod#23225
Blood & Cell Culture DNA Mini Kit	QIAGEN	REF: 13323
FeedBeads Glucose 12mm	Biotech GmbH	Art. No.: SMFB63361
Deposited Data		
Genome sequence data	NCBI	SRP151103 https://www.ncbi.nlm.nih.gov/sra/SRP151103
Experimental Models: Organisms/Strains		
S. cerevisiae, Background: CEN.PK113-5D	Jens Lab	N/A
Oligonucleotides		
For all primers, see Table S2	This paper	N/A
Recombinant DNA		
For all plasmid, see Table S3	This paper	N/A
Software and Algorithms		
Breseq v0.30.2	Deatherage and Barrick, 2014	https://github.com/barricklab/breseq/releases
Bowtie v2.2.8	Langmead and Salzberg, 2012	http://bowtie-bio.sourceforge.net/bowtie2/index.shtml

CONTACT FOR REAGENT AND RESOURCE SHARING

Further information and request for reagents and resources should be directed to and will be fulfilled by the Lead Contact, Jens Nielsen (nielsenj@chalmers.se).

EXPERIMENTAL MODEL AND SUBJECT DETAILS

Strains

Yeast strains for preparation of competent cells were cultivated in YPD consisting of 10 g l^{-1} yeast extract (Merck Millipore, Billerica, MA, USA), 20 g l^{-1} peptone (Difco) and 20 g l^{-1} glucose (Merck Millipore). Strains containing *URA3*-based plasmids or cassettes were selected on synthetic complete media without uracil (SC-URA), which consisted of 6.7 g l^{-1} yeast nitrogen base (YNB) without amino acids (Formedium, Hunstanton, UK), 0.77 g l^{-1} complete supplement mixture without uracil (CSM-URA, Formedium), 20 g l^{-1} glucose (Merck Millipore) and 20 g l^{-1} agar (Merck Millipore). The *URA3* maker was removed and selected against on 5-FOA plates, which contained 6.7 g l^{-1} YNB, 0.77 g l^{-1} CSM-URA and 0.8 g l^{-1} 5-fluoroorotic acid. Shake flask batch fermentations for production of free fatty acids were carried out in minimal medium containing 2.5 g l^{-1} $(NH4)_2SO_4$, 14.4g l^{-1} KH_2PO_4, 0.5 g l^{-1} $MgSO_4 \cdot 7H_2O$, 30 g l^{-1} glucose, trace metal and vitamin solutions supplemented with 60 mg l^{-1} uracil if needed (Verduyn et al., 1992). Cultures were inoculated, from 24 h precultures, at an initial OD_{600} of 0.1 with 15 mL minimal medium in 100mL non- baffled flask and cultivated at 200 rpm, 30°C for 72 h. Glucose feed beads (SMFB63319, Kuhner Shaker, Basel, Switzerland) (Jeude et al., 2006) with a

release rate of 0.25 g l^{-1} h^{-1} were added to the medium to replace the 30 g l^{-1} glucose if needed, and the culture time is 80h for total release the glucose. For nitrogen restricted culture, 1.4 g l^{-1} $(NH4)_2SO_4$ was used. When culture the pdc negative strain, ethanol was used as carbon source. For all engineered strains, see Table S1.

METHOD DETAILS

Implementation of CRISPR/Cas9 system

A *cas9* expression cassette was integrated at the X1-5 site (Mikkelsen et al., 2012) in YJZ045. In detail, the upstream homologous arm X1-5up was amplified from CEN.PK113-5D genomic DNA with primer pair pSOY003/pSOY004. The amplification of the *Kluyveromyces lactis URA3* (*KlURA3*) expression cassette was performed by using primer pSOY005/pSOY006 and pWJ1042 as a template (Reid et al., 2002). The module *TEF1*p-*cas9*-*CYC1*t was amplified from IMX581 genomic DNA with primer pair pSOY007/pSOY008. The downstream homologous arm X1-5 dw was amplified from CEN.PK113-5D genomic DNA with primer pair pSOY009/pSOY010. The whole fragments of X1-5up+(*TEF1*p-*cas9*-*CYC1*t)+*KlURA3*+X1-5 dw was assembled by fusing the DNA parts of X1-5up, *TEF1*p-*cas9*-*CYC1*t, *KlURA3* and X1-5 dw with overlapping PCR. Then, the entire fragment was used to transform YJZ045 and transformants were selected on SC-URA plates. Clones were verified by primer pair pSOY001/pSOY002. Subsequently, 2–3 clones with correct module integration were cultivated overnight in YPD liquid medium and then plated on 5-FOA plates after washing for looping out of the *KlURA3* cassette via homologous recombination between the flanking repeats to obtain strain Y&Z001.

Genetic manipulation by CRISPR/Cas9 system

With the CRISPR/Cas9 system, the deletion of genes and the integration of expression cassettes was performed according to a previously described method (Yu et al., 2017). To select for specific guide RNAs, all potential gRNAs for a given gene were compared with all potential off-targets in the entire CEN.PK113-7D genome using the Yeastriction webtool, which is freely available at http://yeastriction.tnw.tudelft.nl. All gRNA plasmids were constructed following a previously described method (Mans et al., 2015). The construction of the expression cassettes was performed by fusion PCR. The *PYC1* gene was amplified from CEN.PK113-5D genomic DNA by primers pSOY042 and pSOY045. mPYC1 was constructed by adding a mitochondrial localization signal (MLSLRQSIRFFKPATRTLCSSRYLL) sequence by primer pSOY044. The p416GPD-*PYC1* and p416GPD-*mPYC1* plasmids for episomal expression were constructed by Gibson assembly. The native promoters of *ACC1* (from −481 bp to 0 bp) and *PYC1* (from −200 bp to 0 bp) were replaced by the *TEF1* promoter using the CRISPR/Cas9 system. To select for specific guide RNAs for the promoter areas, all potential gRNAs were compared with all potential off-targets in the entire CEN.PK113-7D genome using the CRISPRdirect tool, which is freely available at http://crispr.dbcls.jp/ (Rodriguez et al., 2016b). ACLa and ACLb were amplified from pACLab (Rodriguez et al., 2016b). The native promoter of *PGI1* (from −405 bp to 0 bp) and *IDH2* (from −456 bp to 0 bp) were replaced with relevant fragments. The promoters of *ISU1, ATP14, QCR10, COX9, NAT1, INH1, SDH4, ATP5, GSY1, GSP2, RBK1, GSP1* and *MCM1* were amplified from CEN.PK113-5D genomic DNA. Their sequences were listed in Table S4. The native promoter of *LEU2* (from −195 bp to 0 bp) and *ERG9* (from −138 bp to 0 bp) were replaced by the *HXT1* promoter using the CRISPR/cas9 system. All gRNA plasmids were constructed following a previously described method (Mans et al., 2015). The construction of the expression cassettes was performed by fusion PCR. All primers are listed in Table S2.

Adaptive evolution

The adaptive evolution of Y&Z053 (Y&Z036 *pdc1Δ, pdc5Δ, pdc6Δ*) toward growth on glucose as the sole carbon source were performed in three independent culture lines in 100 mL shake flasks with 15 mL medium at 30°C, which involved two phases. In the first phase, strains were cultivated in minimal medium containing 0.5% glucose and 2% ethanol and then serially transferred every 48 or 72 h using minimal medium with a gradually decreased ethanol concentration and increased glucose concentration for 45 days. Subsequently, the strains were transferred into minimal medium containing 2% glucose as the sole carbon source and evolved for increased growth by serial transfer every 48 or 72 h for 50 days. The three evolved independent culture lines were named as Y&Z054E, Y&Z055E, and Y&Z056E. Single clone isolates were obtained from the Y&Z054, and designated as Y&Z057, Y&Z058, and Y&Z059. Single clone isolates were obtained from the Y&Z055, and designated as Y&Z060, Y&Z061, and Y&Z062. Single clone isolates were obtained from the Y&Z056, and designated as Y&Z063, Y&Z064, and Y&Z065 (Figure S5A).

Genomic DNA Sequencing and Data Analysis

Total genomic DNA of selected strains was extracted by using the Blood & Cell Culture DNA Kit (QIAGEN). Then DNA was prepared using the Illumina TruSeq Nano DNA HT 96 protocol, according to the manufacturer's instructions. The samples were sequenced using an Illumina NextSeq High kit, paired-end 300 cycles (2 × 150 bp). Each sample was represented by 2.2–6.4 million sequence reads. Breseq (Deatherage and Barrick, 2014) 0.30.2 with bowtie (Langmead and Salzberg, 2012) 2.2.8 was used to map the reads of each sample to the genome of *S. cerevisiae* CEN.PK 113-7D (Jenjaroenpun et al., 2018). The option junction-alignment-pair-limit set to 0 (no limit) to ensure all possible new junctions were evaluated. The sequencing data for the initial strain (Y&Z036) was also processed with breseq and used as a reference for removing false-positives from the sample analysis. Briefly, the evidence for each mutation site found in the evolved samples was compared against the same site in the reference strain. If the same type of mutation was present in the same location of the reference strain, then the candidate mutation was discarded as a false-positive. Large-scale

chromosome duplication/deletion were identified by analyzing the coverage maps generated by breseq for each chromosome. All the mutations and genes in chromosome duplication area were listed in Tables S5 and S6.

In vitro enzyme activity assay

The cell was cultured in flask at 0.05. When the OD600 reach 1to 2, samples were centrifuged, washed, and resuspended in potassium phosphate buffer (10mM, pH 7.5, with 2mM EDTA) and stored at −20°C. Before being assayed, samples were thawed, washed, and resuspended in assay buffer from the pyruvate kinase assay kit (abcam). Extracts were prepared with a FastPrep-24 (Nordic biolabs) using 0.75 g glass beads (G8772, Sigma) per ml cell suspension in five bursts (20 s per burst at speed 6, with 5min intervals for cooling). Unbroken cells and debris were removed by centrifugation (4°C, 20min, 21,000*g). the supernatant was used for enzyme activity assays. And the fructose-1,6-bisphosphate (sigma) used as activator if needed. Protein concentrations in the cell extracts were determined by the Pierce BCA protein assay kit (23225, Thermo).

Fed-batch fermentation

The batch and fed-batch fermentations for free fatty acid production were performed in 1.0 l bioreactors, with an initial working volume of 0.25 l, in a DasGip Parallel Bioreactors System (DasGip). The initial batch fermentation was carried out in minimal medium containing 5 g l^{-1} $(NH4)_2SO_4$, 3 g l^{-1} KH_2PO_4, 0.5 g l^{-1} $MgSO_4 \cdot 7H_2O$, 60mg l^{-1} URA, 20 g l^{-1} glucose, trace metal and vitamin solutions. The temperature, agitation, aeration and pH were monitored and controlled using a DasGip Control 4.0 System. The temperature was kept at 30°C, initial agitation set to 800 rpm and increased to maximally 1,200 rpm depending on the dissolved oxygen level. Aeration was initially provided at 36 sl h^{-1} and increased to maximally 48 sl h^{-1} depending on the dissolved oxygen level. The dissolved oxygen level was maintained above 30%, the pH was kept at pH 5.6 by automatic addition of 4 M KOH and 2 M HCl. The aeration was controlled and provided by a DasGip MX4/4 module. The composition of the off-gas was monitored using a DasGip Off Gas Analyzer GA4. Addition of the acid, base, and glucose feed was carried out with DasGip MP8 multi-pump modules (pump head tubing: 0.5 mm ID, 1.0 mm wall thickness). The pumps, pH and DO probes were calibrated before the experiment. During the fed-batch cultivation, the cells were initially fed with a 200 g l^{-1} glucose solution with a feed rate that was exponentially increased ($\mu = 0.05\ h^{-1}$) to maintain a constant biomass-specific glucose consumption rate. The used minimal medium contained 15 g l^{-1} $(NH_4)_2SO_4$, 9 g l^{-1} KH_2PO_4, 1.5 g l^{-1} $MgSO_4 \cdot 7H_2O$, 180 mg l^{-1} uracil, 3 x trace metal and 3 x vitamin solutions. When the volume of the fermentation broth reached 0.4-0.45 l, the feed solution was switched to the following composition: 25 g l^{-1} $(NH_4)_2SO_4$, 15 g l^{-1} KH_2PO_4, 2.5 g l^{-1} $MgSO_4 \cdot 7H_2O$, 300 mg l^{-1} uracil, 600 g l^{-1} glucose, 5 x trace metal and 5 x vitamin solutions (Figures S4D and S4E). For strain Y&Z036, 40ml medium were fed without air supply within 15h at the late phase and then stop feeding with air supply for another 9h to finish the fermentation and show all the potential of this strain (Figure S4D). The initial feed rate was calculated using the biomass yield and concentration that were obtained during prior duplicate batch cultivations with these strains. The feeding was started once the dissolved oxygen level was higher than 30%. Dry cell weight measurements were performed by filtrating 3-5 mL of broth through a weighed 0.45 mm filter membrane (Sartorius Biolab, Göttingen, Germany) and measuring the weight increase after drying for 48 h in a 65°C oven. The filter was washed once before and three times after filtrating the broth with 5 mL deionized water. During fermentation, floating dead cells and fatty acid residues were found to stick to the inner wall or the bottom of the fermenter. After fermentation, all particles were resuspended in the fermentation culture to accurately measure the total FFAs production. Measurements were performed in triplicates.

Metabolite extraction and analysis

FFAs titers in whole-cell culture (only FFAs was measured in this study) were quantified following previously published methods (Zhou et al., 2016). Specifically, 0.2 mL of cell culture (or an appropriate volume of cell culture diluted to 0.2 ml) were transferred to glass vials from 72 h or 80 h incubated cultures, then 10 μL 40% tetrabutylammonium hydroxide (base catalyst) was added immediately followed by addition of 200 μL dichloromethane containing 200 mM methyl iodide as methyl donor and 100 mg l^{-1} pentadecanoic acid as an internal standard. The mixtures were shaken for 30 min at 1,200 rpm by using a vortex mixer, and then centrifuged at 4,000 g to promote phase separation. A 150 μL dichloromethane layer was transferred into a GC vial with glass insert, and evaporated 3 h to dryness. The extracted methyl esters were resuspended in 150 μL hexane and then analyzed by gas chromatography (Focus GC, Thermo Fisher Scientific) equipped with a Zebron ZB-5MS GUARDIAN capillary column (30 m × 0.25mm × 0.25 mm, Phenomenex) and a DSQII mass spectrometer (Thermo Fisher Scientific). The GC program was as follows: initial temperature of 40°C, hold for 2 min; ramp to 130°C at a rate of 30°C per minute, then raised to 280°C at a rate of 10°C per min and hold for 3 min. The temperatures of inlet, mass transfer line and ion source were kept at 280°C, 300°C and 230°C, respectively. The injection volume was 1 μl. The flow rate of the carrier gas (helium) was set to 1.0 mL min^{-1}, and data were acquired at full-scan mode (50–650 m z^{-1}). Final quantification was performed using the Xcalibur software. The yield of extracellular fatty acids was calculated by dividing the mass of the product formed by the total mass of carbon (glucose) supplied at inoculation. Maximum theoretical yield values assumed simplified biochemical reactions as outlined in Varman et al. (2014).

The extracellular glucose, glycerol, ethanol and organic acid concentrations were determined by high-performance liquid chromatography analysis. In detail, a 1.5 mL broth sample was filtered through a 0.2 mm syringe filter and analyzed on an Aminex HPX-87G column (Bio-Rad) on an Ultimate 3000 HPLC (Dionex Softron GmbH). The column was eluted with 5 mM H_2SO_4 at a flow rate of 0.6 mL min^{-1} at 45°C for 26 min.

QUANTIFICATION AND STATISTICAL ANALYSIS

Statistical analysis was performed using one-tailed Student's t-Test (*, $p < 0.05$; **, $p < 0.01$ and ***, $p < 0.001$). The mean ± s. d. for 3 biological replicates in a representative measurement is shown.

DATA AND SOFTWARE AVAILABILITY

The full list of strains, primers and plasmids are available in Tables S1, S2, and S3. The sequences of promoters and codon optimized genes are available in Table S4. The mutations and genes are available in Tables S5 and S6. The accession number for the genome sequence data of evolved strains reported in this paper is [NCBI]: [SRP151103]. See the link: https://www.ncbi.nlm.nih.gov/sra/SRP151103.

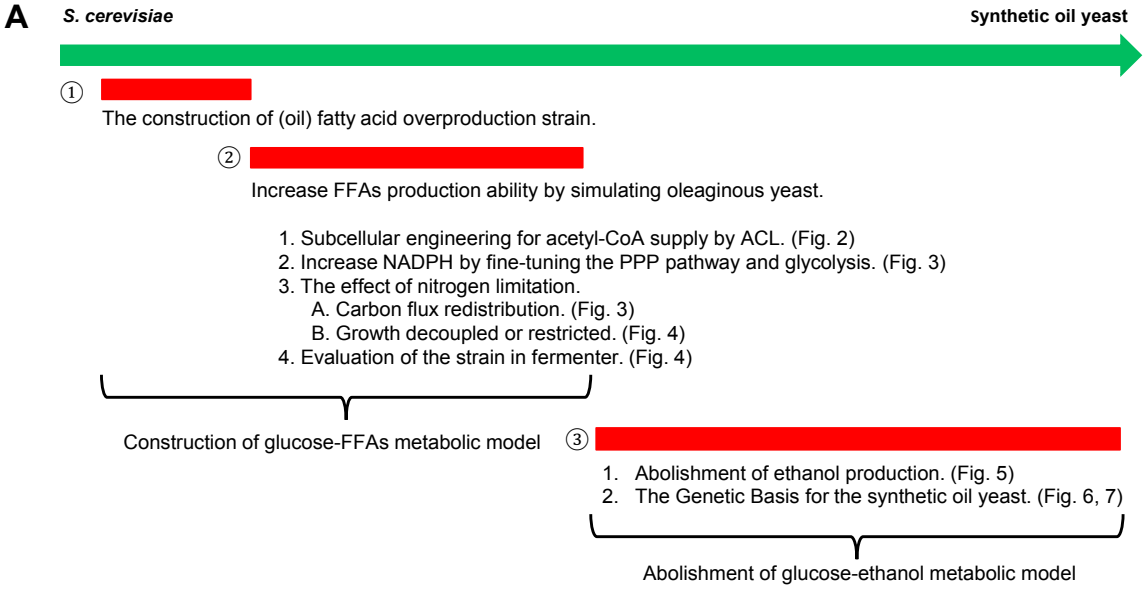

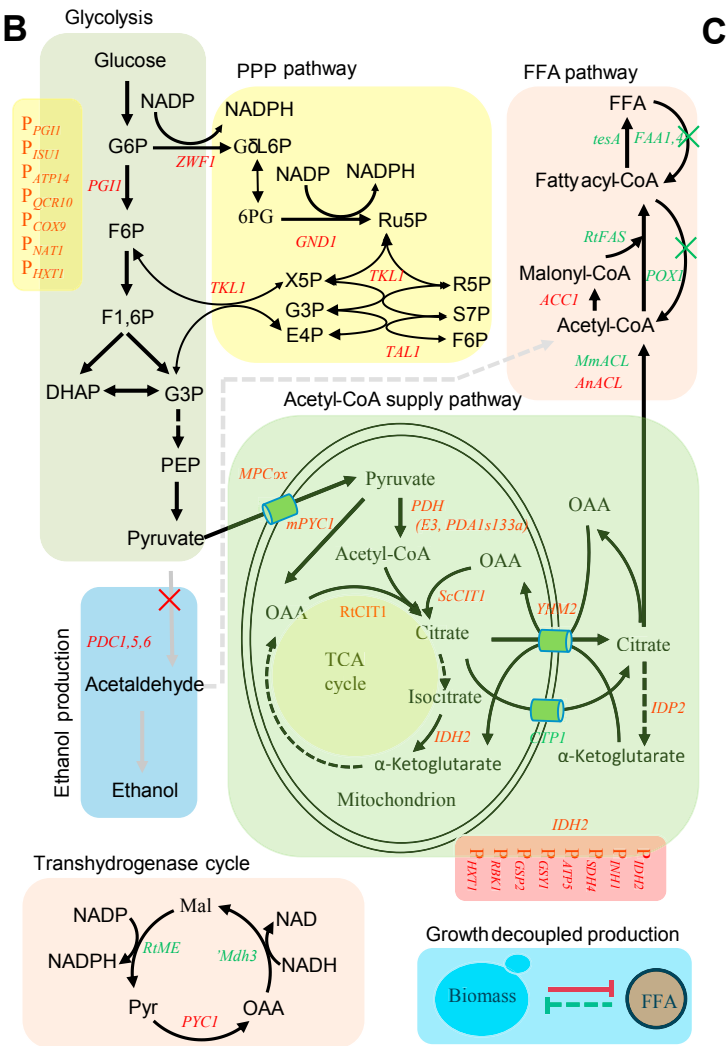

C

Genes	Full name
tesA	the truncated E. coli thioest
MmACL	ATP:citrate lyase from Mus musculus
RtME	cytosolic NADP+-dependent malic enzyme from Rhodosporidium toruloides
'Mdh3	endogenous malate dehydrogenase with removed peroxisomal signal
CTP1	citrate transporter
RtFAS	fatty acid synthase from Rhodosporidium toruloides
FAA1	fatty acyl-CoA synthetase 1
FAA4	fatty acyl-CoA synthetase 4
POX1	fatty acyl-CoA oxidase
MPCox	endogenous mitochondrial pyruvate carrier (MPC1 and MPC3);
RtCIT1	citrate synthase from Rhodosporidium toruloides
AnACL	ATP:citrate lyase from Aspergillus nidulans
PDA1	pyruvate Dehydrogenase Alpha
E3 (LPD1)	dihydrolipoamide dehydrogenase
PGI1	phosphoglucose isomerase
ZWF1	cytoplasmic glucose-6-phosphate dehydrogenase
GND1	the isoform 1 of phosphogluconate dehydrogenase
TKL1	transketolase 1
TAL1	transaldolase 1
IDH2	subunit 2 of mitochondrial NAD(+)-dependent isocitrate dehydrogenase
PYC1	pyruvate carboxylase 1
YHM2	citrate and oxoglutarate carrier protein 2
IDP2	cytosolic NADP-specific isocitrate dehydrogenase 2
ACC1	Acetyl-CoA carboxylase 1
PDC1	pyruvate carboxy 1
PDC5	pyruvate carboxy 5
PDC6	pyruvate carboxy 6
ISU1	IScU homolog 1
ATP14	ATP synthase 14
QCR10	ubiQuinol-cytochrome C oxidoReductase 10
COX9	Cytochrome c Oxidase 9
NAT1	N-terminal AcetylTransferase 1
INH1	Protein that inhibits ATP hydrolysis by the F1F0-ATP synthase 1
SDH4	Membrane anchor subunit of succinate dehydrogenase 4
ATP5	ATP synthase 5
GSY2	Glycogen synthase 1
GSP2	GTP binding protein 2
RBK1	RiBoKinase 1
HXT1	Low-affinity glucose transporter 1

(legend on next page)

Figure S1. Schematic Illustration of All the Modifications in the Strain, Related to Figure 1

(A) Blueprint of the reprograming process. Reprograming *S. cerevisiae* into a FFAs producing yeast: First, the construction of a strain with high FFAs production capacity; Second, increase the FFAs producing ability and set up the new metabolic network, which includes enhancing carbon flux through subcellular engineering, matching the NADPH supply by upregulating the pentose phosphate pathway (PPP) and fine-tuning of ATP supply by downregulating the TCA cycle. Third, abolishing the original metabolic model by removing ethanol fermentation.

(B) The rewired metabolic pathways for synthetic oil yeast. The previously engineered targets in the starting strain YJZ45 are shown in green. The engineering targets from this study are shown in red, to fine tune gene expression, weaker promoters were used.

(C) The annotations of all the genes and promotors in (B).

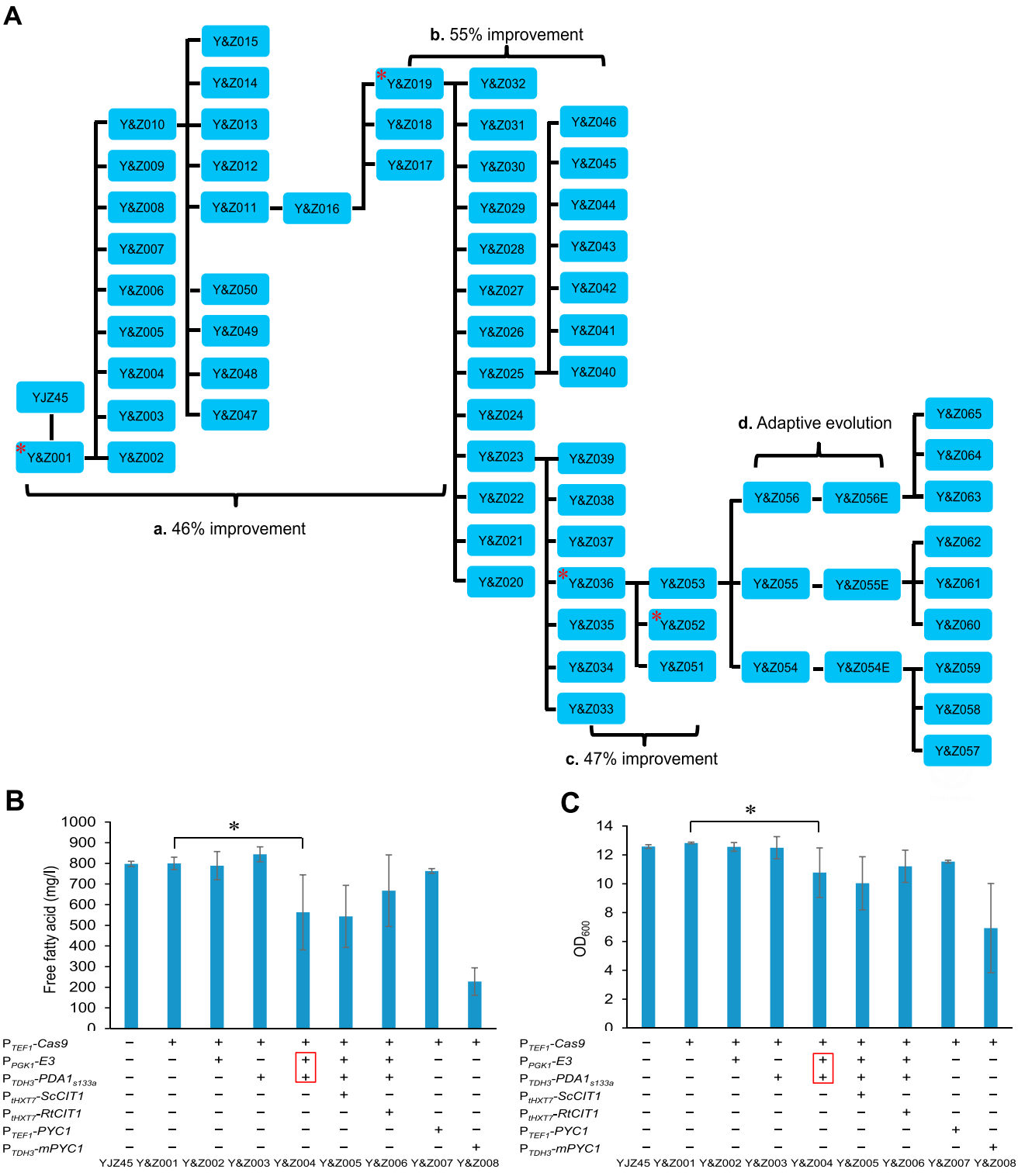

Figure S2. FFA Production Was Impaired by Overexpression of *PDH* Subunit, Related to Figures 1 and 2

(A) Flowchart of yeast strain construction in this study. a. Developed strains in connection to engineering of subcellular metabolic trafficking. From YJZ45 to Y&Z019, the production level was improved by 46%. b. The strains regarding fine-tuning the PPP, TCA cycle and glycolysis. From strain Y&Z019 to Y&Z036, the

(legend continued on next page)

FFAs production ability were improved by 55%. c. Nitrogen restriction improved FFAs production about 47%. d. Adaptive laboratory evolution resulted in the synthetic oil yeast. The key branch point strains were labeled with *.

(B) FFAs production level in the engineered strains.

(C) The cell growth of the strains in (B). FFAs production obtained with engineered strains in shake flasks after 72 h cultivation at 200 rpm, 30°C. Statistical analysis was performed using one-tailed Student's t-Test (*$p < 0.05$; **$p < 0.01$ and ***$p < 0.001$). All data is represented as the mean ± s.d. of biological triplicates.

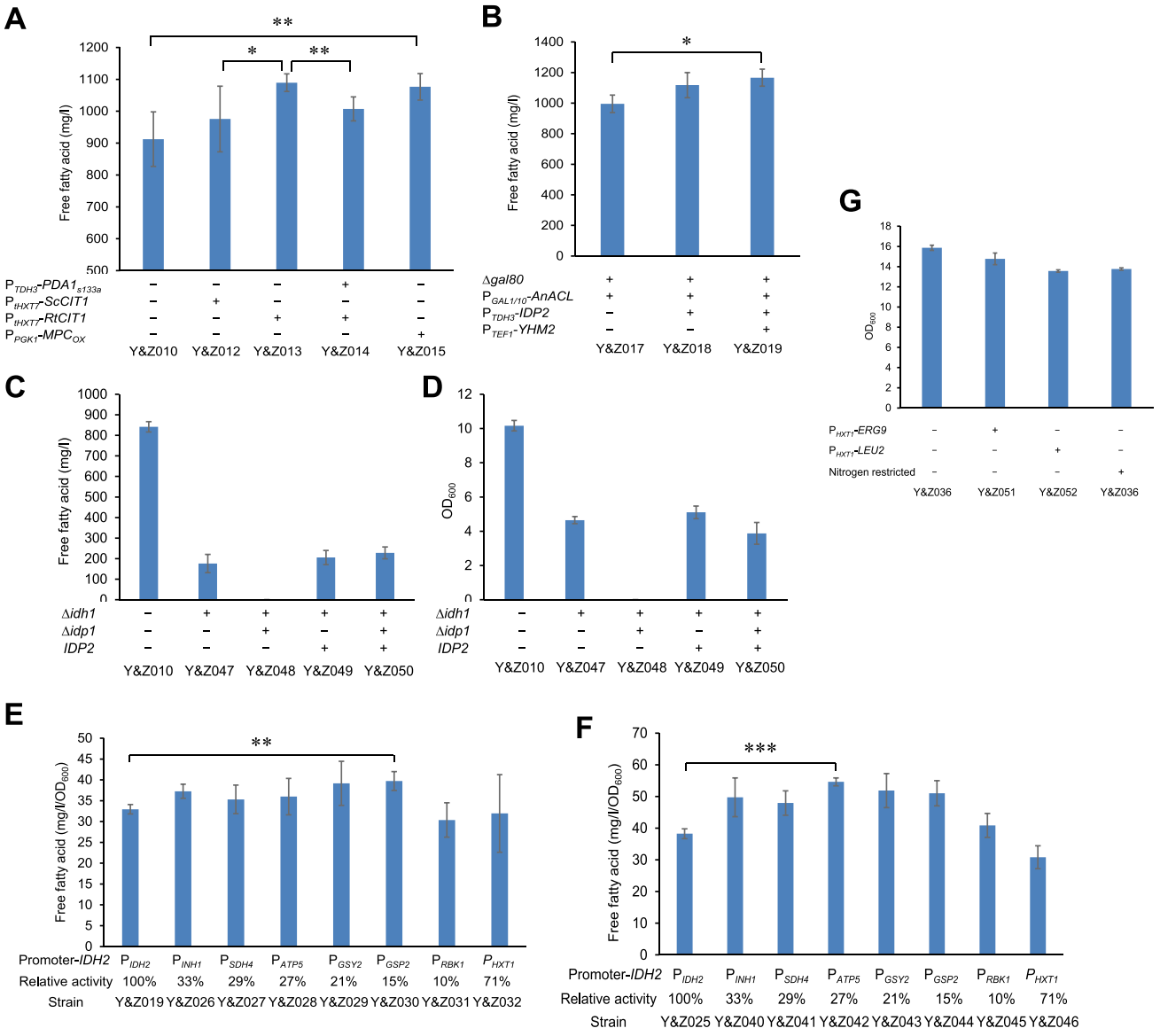

Figure S3. FFA Production Was Increased by Metabolic Engineering, Related to Figures 2, 3, and 4

(A) Metabolite shuttling from cytoplasm into mitochondrion improved FFAs production.

(B) Metabolite shuttling from mitochondrion into cytoplasm improved FFAs production. FFAs production obtained with engineered strains in shake flasks after 72 h cultivation at 200 rpm, 30°C. Statistical analysis was performed using one-tailed Student's t-Test (*$p < 0.05$; **$p < 0.01$ and ***$p < 0.001$). All data is represented as the mean ± s.d. of biological triplicates.

(C) Total channelling of carbon into precursors decreases FFAs production. The deletion of isocitrate dehydrogenase decreases FFAs production due to impaired cell growth.

(D) The cell growth of the strains in (C). FFAs production obtained with engineered strains in shake flasks after 72 h cultivation at 200 rpm, 30°C. All data is represented as the mean ± s.d. of biological triplicates.

(E) Fine tuning of *IDH2* expression for optimized TCA flux improved FFAs production in background strain Y&Z019.

(F) Fine tuning of *IDH2* expression for optimized TCA flux improved FFAs production in background strain Y&Z025. The strains were cultivated in shake flasks for 80h at 200 rpm, 30°C with glucose beads (30 g l^{-1} glucose). The glucose feed beads can release glucose slowly, which will avoid the Crabtree effect. Statistical analysis was performed using one-tailed Student's t-Test (*$p < 0.05$; **$p < 0.01$ and ***$p < 0.001$). All data is represented as the mean ± s.d. of biological triplicates.

(G) The cell growth of the strains with decoupled FFAs production. The strains were cultivated in shake flasks for 80h at 200 rpm, 30°C with glucose beads (30 g l^{-1} glucose and 2.5 g l^{-1} $(NH_4)_2SO_4$). The glucose feed beads can release glucose slowly, which will avoid the Crabtree effect. For nitrogen restricted conditions, 1.4 g l^{-1} $(NH_4)_2SO_4$ was used. All data is represented as the mean ± s.d. of biological triplicates.

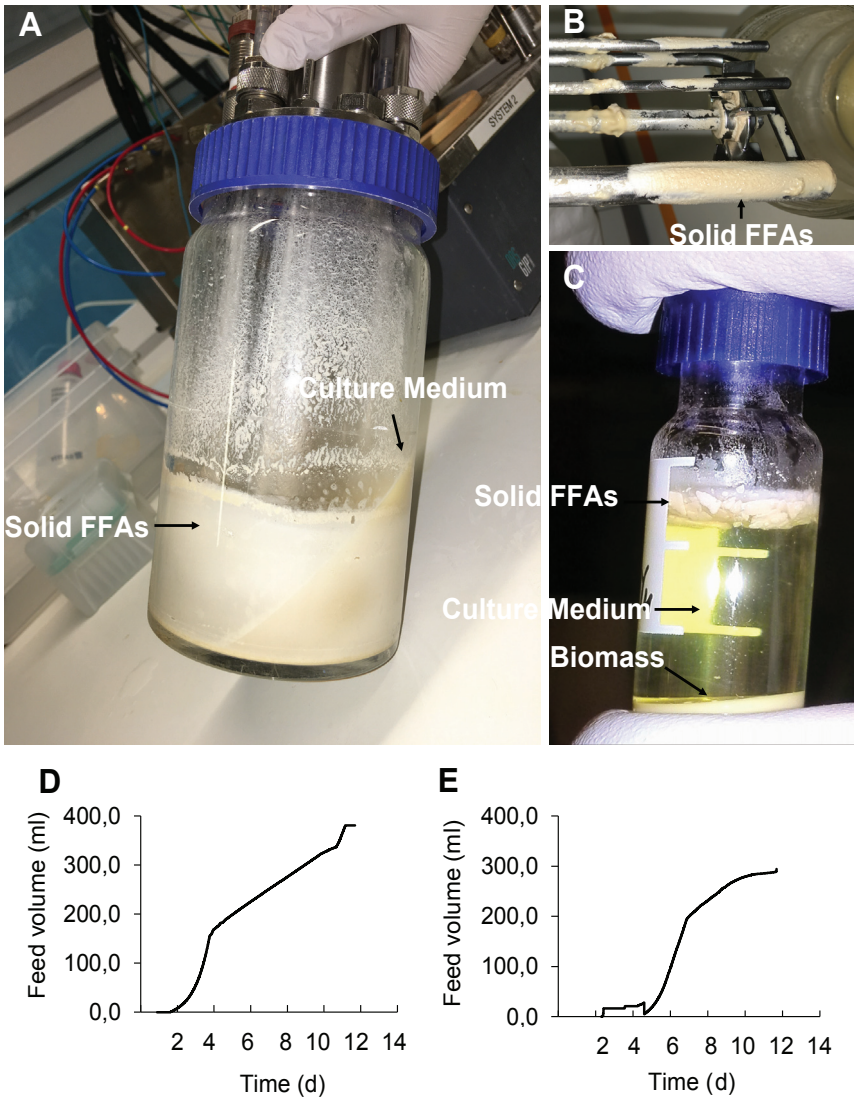

Figure S4. The Solid, Precipitated FFAs after Fermentation, Related to Figures 4 and 5

(A) FFAs precipitated and stuck to the fermenter inner wall during the fermentation.

(B) FFAs stuck to the sensors.

(C) Solid FFAs layer after centrifugation. After fermentation, all particles were resuspended in the fermentation culture, and 1.5ml samples was picked up and centrifuged at 5000 g for 40min.

(D) Feed profile of glucose in the glucose-limited and nitrogen-restricted fermentation process of the strain Y&Z036, Related to Figure 4. During the fed-batch cultivation, the cells were initially fed with a 200 g l^{-1} glucose solution with a feed rate that was exponentially increased to maintain a constant biomass-specific glucose consumption rate. Then, glucose feeding speed is based on the dissolved oxygen level. The Nitrogen limitation was achieved by changing into low Nitrogen feed solution.

(E) Feed profile of glucose in the glucose-limited and nitrogen-restricted fermentation process of the synthetic oil yeast strain Y&Z055E, Related to Figure 5. During the fed-batch cultivation, the cells were initially fed with a 200 g l^{-1} glucose solution with a feed rate that was exponentially increased to maintain a constant biomass-specific glucose consumption rate. Then, glucose feeding speed is based on the dissolved oxygen level. The Nitrogen limitation was achieved by changing into low Nitrogen feed solution.

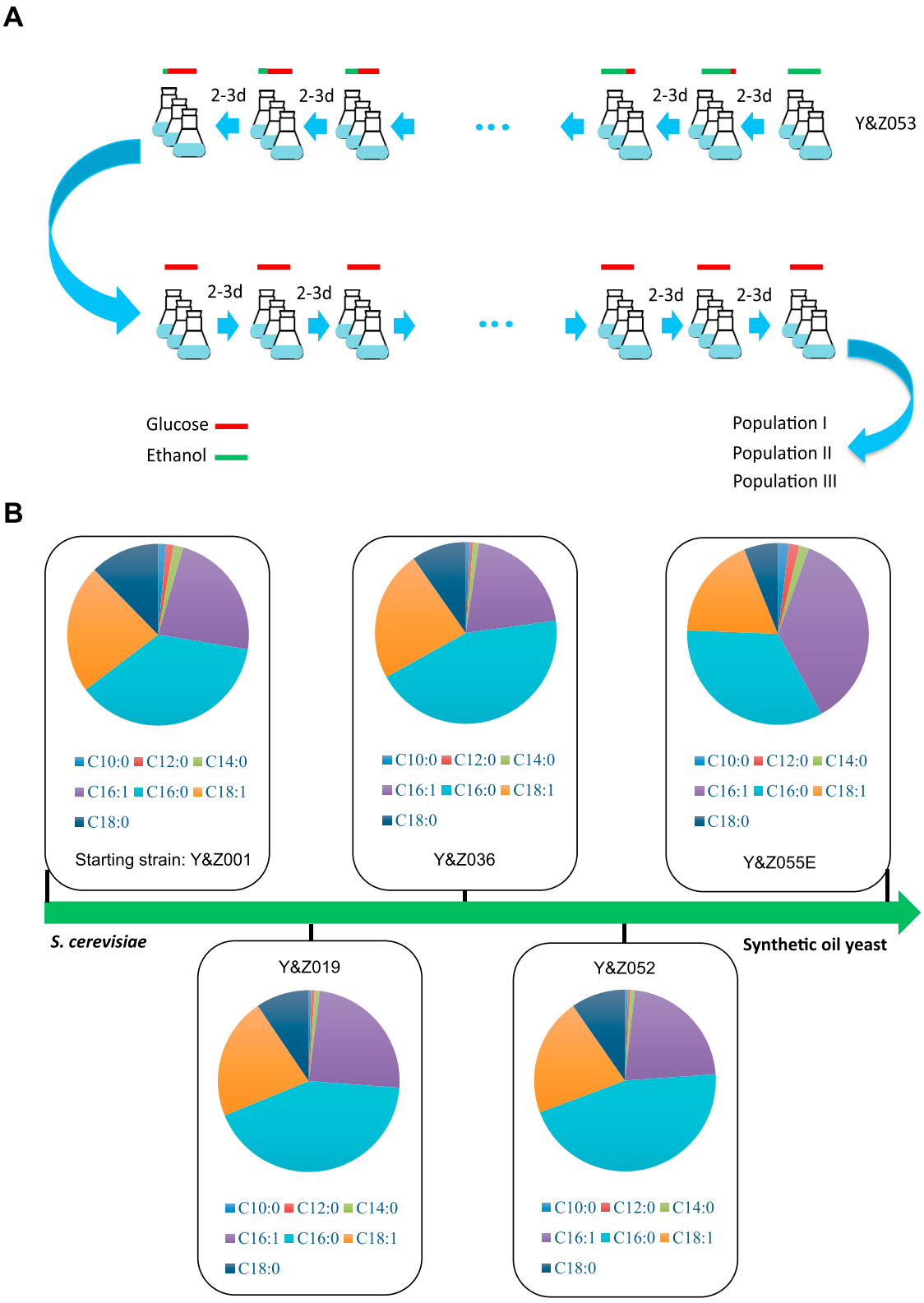

Figure S5. The Change of FFAs Profiles and Adaptive Evolution Process, Related to Figure 5

(A) Adaptive Evolution Process of the pdc negative synthetic oil strain. Three single colonies were picked up from strain Y&Z053 and re-named as Y&Z054, Y&Z055 and Y&Z056. They are evolved in three separated flasks. The strains were cultivated in minimal medium containing 0.5% glucose and 2% ethanol and

(legend continued on next page)

then serially transferred every 48 or 72h using minimal medium with a gradually decreased ethanol concentration and increased glucose concentration for 45 days. Subsequently, the strains were transferred into minimal medium containing 2% glucose as the sole carbon source and evolved for increased growth by serial transfer every 48 or 72h for another 50 days. After evolution, they were labeled as population I, population II, and population III.

(B) The change of FFAs profiles during the reprogramming process. Y&Z001: the starting strain. Y&Z019: the strain with increased supply of the cytosolic acetyl-CoA (see Figure 2). Y&Z036: the strain with fine-tuning of the PPP pathway, TCA cycle and glycolysis (see Figure 3). Y&Z052: the strain with growth restricted design (see Figure 4). Y&Z055E: the evolved Synthetic oil yeast (see Figure 5).

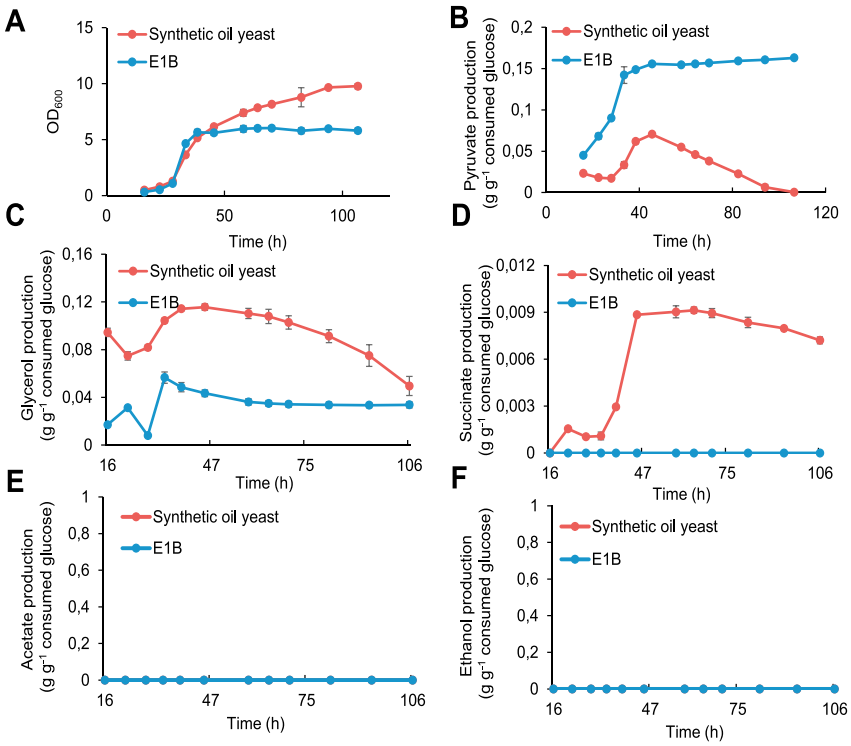

Figure S6. Batch Culture of the Synthetic Oil Yeast Strain Y&Z055E and E1B Strain, Related to Figure 5 and 7

(A–F) Time courses of OD_{600} value (A), pyruvate (B), glycerol (C), succinate (D), acetate (E), and ethanol (F) in batch culture. Fermentation product profiles obtained with engineered strains in shake flasks during 5d cultivation at 200 rpm, 30°C with 30 g l^{-1} glucose. All data represent the mean ± s.d. of biological triplicates.

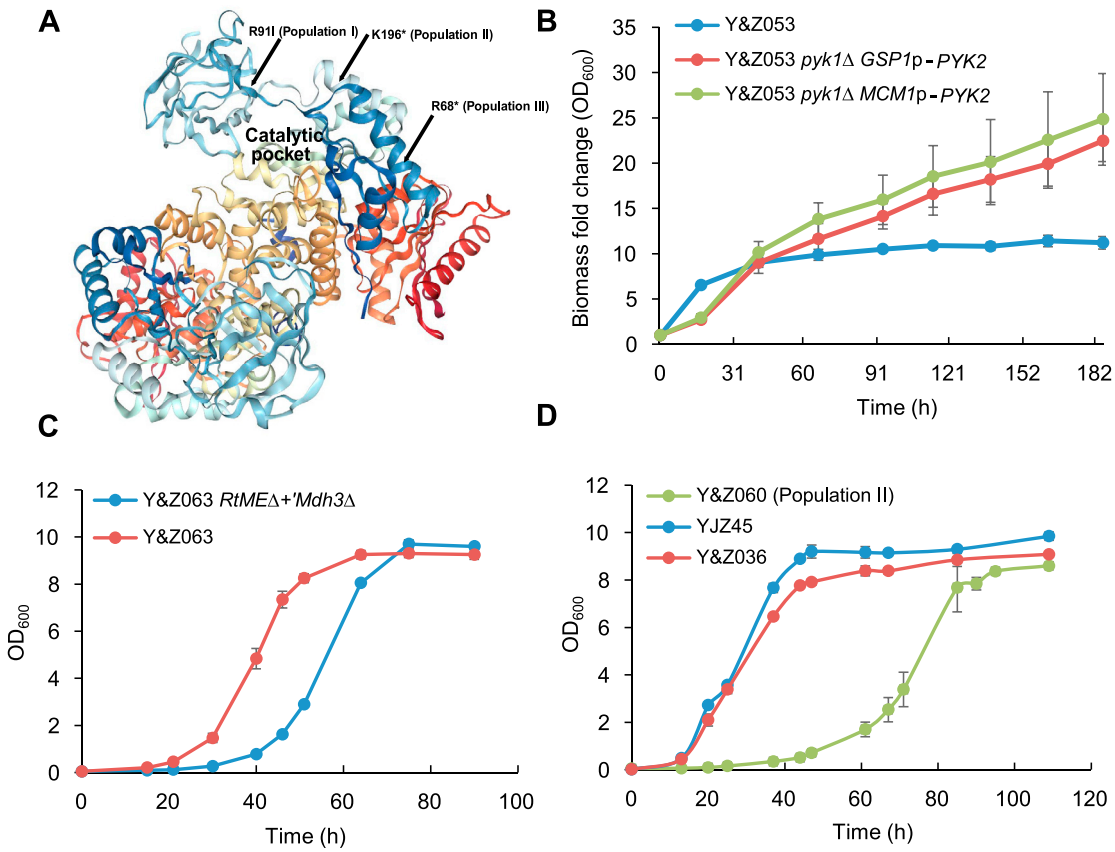

Figure S7. The Cell Growth of Key Strains, Related to Figure 6 and 7

(A) The structure of *PYK1* and the mutations. Pyruvate kinase (Pyk1), converting phosphoenolpyruvate (PEP) and ADP to pyruvate and ATP, is one of the major control points of glycolysis. Structural analysis indicates that the mutations are close to catalytically pocket regions of the enzyme, either as stop codon.

(B) Downregulation of pyruvate kinase enabled the growth of pdc negative strain in high concentration of glucose. The strains were cultured in shake flasks at 200 rpm, 30°C with 20 g/L glucose and 0.5% (v/v) ethanol. All data represent the mean ± s.d. of biological triplicates. The activity of *GSP1* promoter is almost 30% of the native *PYK1* promoter, 6-fold of native *PYK2* promoter. The activity of *MCM1* promoter is almost 15% of the native *PYK1* promoter, 3-fold of native *PYK2* promoter. The *PYK1* gene was deleted in Y&Z053, then a *PYK2* gene under the promoter of *GSP1* or *MCM1* in a low plasmid was introduced into the cell to get the strain Y&Z053 *pyk1Δ GSP1p-PYK2* or Y&Z053 *pyk1Δ MCM1p-PYK2*. (*GSP1*, Ran GTPase; *MCM1*, Sequence-specific DNA-binding RNA polymerase II transcription activator and repressor)

(C) Deletion of transhydrogenase cycle decreased the cell growth of evolved strain Y&Z063. The transhydrogenase cycle can transform NADH into NADPH, which contains *PYC1*, *RtME* and *'Mdh3*. The strains were cultured in shake flasks at 200 rpm, 30°C with 20 g/L glucose. All data represent the mean ± s.d. of biological triplicates. The initial OD600 value is 0,1. See also Figure S1.

(D) The growth curve of the evolved strain Y&Z060, the parents strain Y&Z036 and the initial strain YJZ045. The strains were cultured in shake flasks at 200 rpm, 30°C with 20 g/L glucose. All data represent the mean ± s.d. of biological triplicates. The initial OD600 value is 0,025.